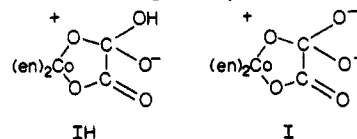


with $[\text{Co}(\text{en})_2(\text{O}_2\text{C}_2\text{O}_2)]^+$ being stable for at least 1 year in 1 mol dm^{-3} hydrochloric acid. Acid-catalyzed exchange of the two exocyclic oxygens, however, does occur ($k_{\text{ex}} = 2.3 \times 10^{-5} \text{ mol}^{-1} \text{ dm}^3 \text{ s}^{-1}$), and there is some suggestion of a much slower exchange of the chelated oxygens.¹⁶ The faster process has been attributed to loss of water from the intermediate IH_3 .¹⁶

In neutral conditions cyclization of $\text{cis-}[\text{Co}(\text{en})_2(\text{OC}_2\text{O}_3)(\text{OH}_2)]^+$ occurs by loss of water from either carboxylate carbon or the metal. The former reaction is some 10 times slower than that found for $\text{cis-Co}(\text{en})_2(\text{OC}_2\text{O}_3\text{H})(\text{OH}_2)]^{2+}$. A similar rate difference was found between the aqua glycinate $\text{cis-}[\text{Co}(\text{en})_2(\text{glyO})(\text{OH}_2)]^{2+}$ and aqua glycine acid $\text{cis-}[\text{Co}(\text{en})_2(\text{glyOH})(\text{OH}_2)]^{3+}$ where the reaction occurs entirely by attack of coordinated water at the carbon center.¹⁴ The more rapid cyclization in the glycine system avoids water exchange at the metal, and it is this latter process which allows competitive entry of carboxylate in the oxalate system. Water exchange at the metal is likely to dominate all slow cyclization processes.

In more alkaline conditions where ionization of coordinated water has occurred, cyclization of $[\text{Co}(\text{en})_2(\text{OC}_2\text{O}_3)(\text{OH})]$ is relatively unimportant; hydrolysis of the ligand is preferred. A similar, although not identical, situation is found with the glycinate system with cyclization of $\text{cis-}[\text{Co}(\text{en})_2(\text{glyO})(\text{OH})]^+$ being at least 100 times slower than for $\text{cis-}[\text{Co}(\text{en})_2(\text{glyO})(\text{OH}_2)]^{2+}$. It is not known whether the latter reaction occurs via attack at the metal center by carboxylate oxygen or by coordinated hydroxide attack at carboxylate carbon,¹⁴ but the slower complete loss of N-bound monodentate glycinate in alkaline solution compared to monodentate oxalate allows cyclization to occur. Attack by coordinated hydroxide is found at the ester²⁷ and amide²⁹ carbon, with both OH^- -independent and OH^- -dependent paths contributing to the rate. Similar paths to IH or I from $\text{cis-}[\text{Co}(\text{en})_2(\text{OC}_2\text{O}_3)(\text{OH})]$ would accommodate the observed O-exchange into the endocyclic oxygens of $[\text{Co}(\text{en})_2(\text{O}_2\text{C}_2\text{O}_2)]^+$, and an analysis of the data requires $(k_{-3}' + k_{-4}')$ to be $\leq 10^{-3} \text{ s}^{-1}$ in 1.0 mol $\text{dm}^{-3} \text{ OH}^-$. The alternative possibility of switching of O atoms in IH by rotation about the C-C bond³² is considered unlikely.

Microscopic reversibility requires a path for cyclization via displacement of coordinated hydroxide since hydrolysis of $[\text{Co}(\text{en})_2(\text{O}_2\text{C}_2\text{O}_2)]^+$ shows some OH^- -catalyzed displacement at the metal. However OH^- -catalyzed hydrolysis of the monodentates to give $\text{cis-}[\text{Co}(\text{en})_2(\text{OH})_2]^+$ is preferred in these circumstances. The deprotonated intermediates IH and I lead exclusively to cleavage in the chelate ring. Only intermediate IH is required



for O-exchange. Probably CoO-C bond fission occurs via solvent protonation of the bound oxygen atom since CoO^- does not provide an acceptable leaving group in water.

Hydrolysis of both the *cis* and *trans* monodentates occurs via Co-O bond fission. This is easily reconciled in terms of the commonly encountered $\text{S}_{\text{N}}1(\text{CB})$ mechanism for hydrolysis via a deprotonated ethylenediamine precursor.

The above comments could well be of general applicability to cobalt(III) carboxylate systems. Differences will result from variations in the acidity of the monodentate carboxylate or coordinated water functions and possibly from more substantial variations in the rates of water or hydroxide exchange at the metal. Attack at carboxylic acid carbon by coordinated water, or at carboxylate carbon by coordinated hydroxide, should not be appreciably affected by the other ligands on the metal, but this aspect has yet to be tested.

Acknowledgment. We thank Dr J. Hulston, Institute of Nuclear Sciences, D.S.I.R., Lower Hutt, for measurement of oxygen isotopic ratios.

Registry No. *cis-}[\text{Co}(\text{en})_2(\text{OC}_2\text{O}_3)(\text{OH}_2)]\text{PF}_6, 102920-52-5; *cis-}[\text{Co}(\text{en})_2(\text{OC}_2\text{O}_3)(\text{OH})], 59982-23-9; *cis-}[\text{Co}(\text{en})_2(\text{OC}_2\text{O}_3)(\text{OH}_2)]^+, 87036-83-7; *cis-}[\text{Co}(\text{en})_2(\text{OC}_2\text{O}_3\text{H})(\text{OH}_2)]^{2+}, 102920-53-6; $[\text{Co}(\text{en})_2(\text{O}_2\text{C}_2\text{O}_2)]^+$, 17835-71-1.****

Supplementary Material Available: Listings of observed reaction products (Table III) and rate data for hydrolysis (Table II) and cyclization (Table IV) (5 pages). Ordering information is given on any current masthead page.

(32) Broomhead, J. A.; Kane-Maguire, N.; Lauder, I.; Nimmo, P. *J. Chem. Soc., Chem. Commun.* 1968, 747.

(31) Dash, A. C.; Nanda, R. K.; Ray, N.; Rout, K. C. *Int. J. Chem.* 1984, 23A, 907. These authors obtained a curved plot with zero intercept when k_{obsd} was plotted against $[\text{OH}^-]$ and a linear plot, interpreted as $k_{\text{obsd}} = k_0 + k_2[\text{OH}^-]^2$ when k_{obsd} was plotted against $[\text{OH}^-]^2$; the two are in obvious disagreement. From plots of $k_{\text{obsd}}/[\text{OH}^-]$ vs. $[\text{OH}^-]$ or when a least-squares quadratic fit is used, the rate law $k_{\text{obsd}} = k_1[\text{OH}^-] + k_2[\text{OH}^-]^2$ is obtained for all the data.

Design and Synthesis of a New Ferroelectric Liquid Crystal Family. Liquid Crystals Containing a Nonracemic 2-Alkoxy-1-propoxy Unit

David M. Walba,^{*1a,c} Stacey C. Slater,^{1a} William N. Thurmes,^{1a} Noel A. Clark,^{*1b,d} Mark A. Handschy,^{1b} and Frank Supon^{1b}

Contribution from the Department of Chemistry and Biochemistry and Department of Physics, University of Colorado, Boulder, Colorado 80309. Received January 16, 1986

Abstract: The synthesis and phase behavior of a new class of nonracemic liquid crystal materials of general structure 1, possessing a phenyl benzoate core and chiral nonracemic 2-alkoxy-1-propoxy tail unit derived from ethyl acetate, are described. Several of the new materials possess monotropic ferroelectric liquid crystal (FLC) phases at or near room temperature. These materials exhibit the fastest room temperature electro-optical switching characteristics of any known FLC's. A discussion of the ferroelectric polarization in nonracemic tilted smectic liquid crystal phases is given. It is suggested that the phenomenon may be considered in terms of a novel kind of molecular recognition occurring in the liquid crystal phase.

Phenomena involving molecular recognition in complexation have long been of great interest in organic chemistry, and con-

siderable current research is directed toward understanding and utilizing molecular recognition in chemical aggregates. In its

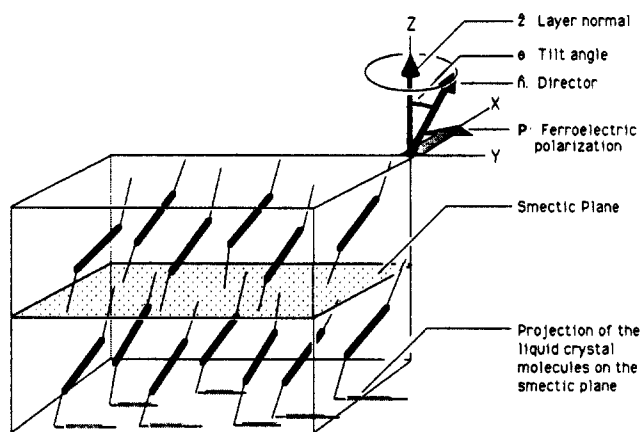


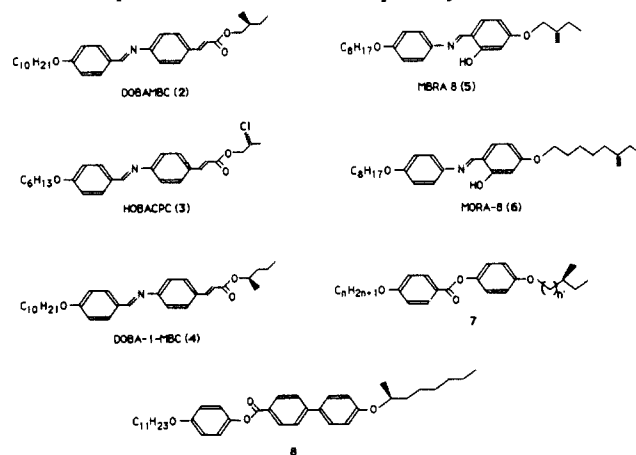
Figure 1. The smectic C phase.

broadest sense, this area includes host-guest chemistry between solutes in solution,² crystalline host-guest complexation (clathrate design),³ the study of reactions occurring in crystalline solids,⁴ resolution of racemates by crystallization of diastereomeric salts,⁵ the study of polar crystals,⁶ chiral aggregation phenomena occurring in nonracemic ordered liquid phases such as lipid bilayers⁷ and cholesteric liquid crystal phases,⁸ and study of differences in physical properties of racemic and enantiomerically pure liquids.⁹ Applications of this work include novel methods for determination of enantiomeric purity and resolution of racemates and unique approaches to asymmetric induction in organic reactions.

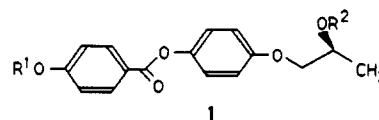
Recently, some potentially very useful properties of the tilted smectic C liquid crystal phases composed of chiral, nonracemic molecules have been described.¹⁰ In particular, tilted chiral smectic phases possess a spontaneous *ferroelectric polarization*, or macroscopic dipole moment, deriving from a dissymmetry in the orientation of molecular dipoles in the liquid crystal phase. This type of behavior, while quite common in crystalline solids,⁶ until very recently was unknown in liquid or liquid crystal phases.

The ferroelectric polarization of tilted chiral smectic phases may be considered a manifestation of molecular recognition occurring in an ordered liquid and seems closely related to other molecular aggregation phenomena of high current interest to the chemical community. In this paper we describe work aimed at achieving a basic understanding of the origins of the ferroelectric polarization in chiral smectic C phases (hereafter simply referred to as C* phases) and development of methods for design of new ferroelectric liquid crystal materials with specific properties. In particular, the synthesis and some properties of a new class of

Chart I. Representative Ferroelectric Liquid Crystals



ferroelectric liquid crystal (FLC) materials possessing a nonracemic 2-alkoxy-1-propoxy tail unit, as shown in structure 1, is



described. Data on the phase behavior of the new compounds is given, and a general stereochemical model for the ferroelectric polarization of C* materials is proposed. We begin with a discussion of tilted smectic liquid crystals, the symmetry argument for ferroelectricity of C* phases, and some aspects of molecular structure which influence the design of FLC's.

Ferroelectric Smectic C Liquid Crystals. In the smectic C liquid crystal phase, rod-shaped molecules possess ordering such that in the time average (1) the molecules are arranged in planes; (2) the molecular long axes are orientationally ordered, the mean orientation given by a unit vector \hat{n} (the *director*); (3) the director is *tilted* with respect to the smectic planes; and (4) within the smectic C planes, the centers of mass of the molecules are organized as two-dimensional liquids. The smectic C phase is nonpolar, there being disorder with respect to end for end flips about the molecular short axes. Thus, all properties of the smectic C phase are invariant with sign reversal of \hat{n} .

Figure 1 depicts a small three-dimensional slice cut out of a smectic C phase. Two layers are shown, and the important unit vectors \hat{z} (the *layer normal*) and \hat{n} are indicated. The angle between \hat{z} and \hat{n} is the smectic tilt angle θ , and the plane containing both \hat{z} and \hat{n} is the *tilt plane*.

The time average symmetry of such a smectic phase when the molecules are achiral or the material is racemic is C_{2h} , with a C_2 axis normal to the tilt plane (along the x axis in Figure 1),¹¹ and a mirror plane parallel to the tilt plane. In 1974 Meyer realized that if the molecules of a smectic C phase were chiral and nonracemic, then the symmetry of the phase would be C_2 , since the mirror plane would no longer be present.¹² The low symmetry of such a phase allows for spontaneous formation of a permanent, macroscopic dipole moment, the ferroelectric polarization P , of the phase along the C_2 axis, as shown in Figure 1. In collaboration with Meyer, chemists Keller, Liébert, and Strzelecki prepared the nonracemic C* FLC material p -[[decyloxy]benzylidene)-

(11) Actually, the smectic C phase composed of achiral or racemic material is assigned C_{2h} symmetry specifically because no such phase has ever been observed to possess a spontaneous ferroelectric polarization. There is however no fundamental reason why molecules with the symmetry of an arrow cannot align in the phase with the arrow heads oriented in a preferred direction, in which case *properties of the phase would not be invariant with sign of the director*. This, of course, would break the C_2 symmetry element of an achiral C phase and could result in a ferroelectric polarization along \hat{n} . Indeed, if this sort of ordering could occur in liquid crystal phases, simple chiral or achiral nematics or any other liquid crystal phase could be ferroelectric. Such behavior has yet to be observed in real materials.

(12) Meyer, R. B., presented at the Vth International Liquid Crystal Conference, Stockholm, 1974.

(1) (a) Department of Chemistry and Biochemistry. (b) Department of Physics. (c) Dreyfus Teacher-Scholar, 1984-1986. (d) Fellow of the John Simon Guggenheim Foundation, 1985-1986.

(2) (a) Cram, D. J.; Cram, J. M. *Science* (Washington, DC) **1974**, *183*, 803. (b) Cram, D. J.; Cram, J. M. *Acc. Chem. Res.* **1978**, *11*, 8-14. (c) Cram, D. J.; Trueblood, K. N. *Top. Curr. Chem.* **1981**, *98*, 43. (d) Lehn, J. M. *Struct. Bonding* **1973**, *16*, 1-69. (e) Lehn, J. M. *Pure Appl. Chem.* **1977**, *49*, 857-870. (f) Lehn, J. M. *Acc. Chem. Res.* **1978**, *11*, 871-892. (g) Vögtle, F.; Sieger, H.; Müller, W. M. *Top. Curr. Chem.* **1981**, *98*, 107.

(3) For excellent recent discussions of many aspects of crystalline host-guest chemistry and also host-guest chemistry in solution, see: *Inclusion Compounds*; Attwood, J. L., Davies, J. E. D., MacNicol, D. D., Eds.; Academic Press: London, England, 1984; Vol. 1-3.

(4) Addadi, L.; Berkovitch-Yellin, Z.; Weissbuch, I.; Van Mil, J.; Shimon, L. J. W.; Lahav, M.; Leiserowitz, L. *Angew. Chem.* **1985**, *97*, 476-96.

(5) Jacques, J.; Wilen, S.; Collet, A. *Enantiomers, Racemates & Resolutions*; Wiley-Interscience: New York, 1981.

(6) (a) Patil, A. A.; Curtin, D. Y.; Paul, I. C. *J. Am. Chem. Soc.* **1985**, *107*, 726-727. (b) Duesler, E. N.; Kress, R. B.; Lin, C.; Shiao, W.-I.; Paul, I. C.; Curtin, D. Y. *Ibid.* **1981**, *103*, 875-879.

(7) See, for example: (a) Arnett, E. M.; Gold, J. M. *J. Am. Chem. Soc.* **1982**, *104*, 636-639. (b) Tsai, M. D.; Jiang, R. T.; Bruzik, K. *Ibid.* **1983**, *105*, 2478-2480.

(8) Solladie, G.; Zimmermann, R. *Angew. Chem., Int. Ed. Engl.* **1985**, *24*, 64.

(9) Herndon, W. C.; Vincenti, S. P. *J. Am. Chem. Soc.* **1983**, *105*, 6174-6175.

(10) Meyer, R. B.; Liébert, Strzelecki, L.; Keller, P. *J. Phys. (Les Ulis, Fr)* **1975**, *36*, L-69.

amino]-2-methylbutyl-cinnamate (DOBAMBC, **2**, Chart I), and the ferroelectric properties of such phases were first demonstrated.¹⁰

It can be similarly argued that isotropic liquids, nematic liquid crystals, and indeed any untilted layered liquid crystal phase composed of chiral nonracemic molecules are *not* required to possess a spontaneous polarization.¹¹ On the other hand, any of a variety of the tilted liquid crystal phases besides the C* will in general possess a nonzero polarization. The C* phase is the least ordered of all liquid crystal phases possessing a spontaneous polarization (smectics C*, F*, I*, G*, H*, J*, and K*).¹³

While locally (say on the scale of ten smectic layers) the C* phase has a ferroelectric polarization, globally (i.e., in a macroscopic sample of the material) there is no dipole for the following reason. In the general case, the director \hat{n} in a C* phase will "precess" about the layer normal \hat{z} in passing through the layers (up to down in Figure 1). This precession forms a helical periodicity with a pitch which is long compared to the layer spacing. This helical variation of the director in the smectic phase is analogous to the helical variation in the director in the well-known chiral nematic (cholesteric) phases. The polarization vector therefore rotates about the layer normal as one passes normal to the layers through the material, and the ferroelectric polarization averages to zero in a bulk sample.

The Surface-Stabilized Ferroelectric Liquid Crystal (SSFLC) Device Concept. While very interesting, ferroelectric liquid crystal phases might have remained novel laboratory objects but for some interesting potential practical applications of the materials. Specifically, Clark and Lagerwall have recently described the SSFLC light modulation device concept based upon the use of ferroelectric smectic liquid crystal phases.¹⁴

In the SSFLC cell, a C* material is introduced between two glass plates with surface treatment such that the molecules arrange themselves with the director parallel to the glass plates and the smectic planes perpendicular to the plates. If the LC layer is thin relative to the helical pitch of the phase (i.e., about 2 μm thick), then the helix will be spontaneously "unwound" by the surface interactions, and the director will assume a nonhelical orientation.

In addition, it is often possible to further orient the smectic layers such that they are flat and parallel. Thus, the entire cell can be uniformly oriented to produce a homogeneous material which behaves optically much like a uniaxial crystal. The drawing in Figure 1 would represent a slice of this phase where the glass plates are parallel to the tilt plane and normal to the smectic layers. Under these conditions, the molecules in the entire macroscopic sample (about 1–3 μm thick and up to many cm square) could be oriented as shown in Figure 1.

With the phase oriented in an SSFLC cell, the ferroelectric polarization vector \mathbf{P} will be perpendicular to the glass plates. In Figure 1, a polarization vector is indicated pointed back behind the plane of the paper (\mathbf{P} points from $-$ to $+$). The polarization is an intrinsic property of the material making up the phase and has a certain *magnitude* (the ferroelectric polarization per unit area P) and *sign* for a given material under a given set of conditions. By convention, if the polarization points back when the director tilts to the right, as shown in Figure 1, then \mathbf{P} is *positive*. This is simply an application of the right hand rule; that is, with the orientation of \hat{z} and \hat{n} chosen such that $\hat{z} \cdot \hat{n}$ is positive, if \mathbf{P} is in the direction of the vector $\hat{z} \times \hat{n}$, then the polarization is positive. If \mathbf{P} is opposed to the cross product $\hat{z} \times \hat{n}$, then the polarization is negative. In general, P and θ are temperature dependent, and both increase with decreasing temperature.

In the SSFLC cell, for a given material there may be two stable states of the director field, separated by a barrier resulting from surface interactions (in general, there are more than two states). In the two-state case the states result from the two possible orientations of the director parallel to the surface. Figure 2 depicts the phase looking down the C_2 axis. The plane of the paper is

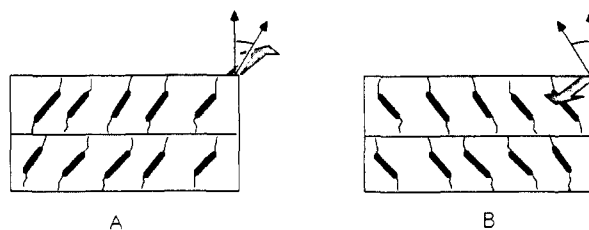


Figure 2. Two stable states of an SSFLC cell.

thus the tilt plane and also represents the plane of the glass plates. In (Figure 2) A the director tilts right. For a material with positive polarization, \mathbf{P} would be pointing back, behind the plane of the paper. In (Figure 2) B the director tilts left. The same material in this state would have its polarization vector aiming straight up, out of the plane of the paper. Both states A and B (in Figure 2) have equal energies in the absence of an externally applied field.

In the presence of an applied field perpendicular to the glass plates, one orientation becomes favored—that with \mathbf{P} aligned with the field—and the molecules will "switch" to align \mathbf{P} with the field if it is not aligned. This switching (e.g., from state A to B (in Figure 2)) has a *threshold*.¹⁴ That is, when a field below a characteristic threshold value is applied, no switching is observed. When a field above the threshold is applied, switching between states occurs. When the field is removed, the molecules will remain in that state until the opposite field is applied. This latter property is termed *orientational bistability*. Within a large range of electric field strengths, the optical rise time τ (s, 10% \rightarrow 90% optical response following an applied voltage step) is inversely proportional to applied field strength, as indicated in eq 1, where P is the ferroelectric polarization density (magnitude of the polarization vector \mathbf{P} , is esu/cm²), η is the orientational viscosity (in poise or dyne-s/cm²), and E is the applied field (dynes/esu).¹⁵

$$\tau \approx \eta / (PE) \quad (1)$$

Though the liquid crystal layer in the Clark–Lagerwall cell is very thin (on the order of 1–3 μm), it is sufficiently birefringent to produce useful optical effects based on the different propagation characteristics of polarized light in the two states. Indeed, if the cell is fitted with crossed polarizers (in front and back), switching between black and clear is possible, affording a light valve with contrast comparable or superior to that obtained with the currently popular twisted nematic liquid crystal watch displays and the new generation of LCD computer displays. In addition, due to the relatively strong coupling between the geometry of the FLC phase and the externally applied field, the theoretical limit for electrooptic switching time τ in the Clark–Lagerwall cell may be estimated as 10–50 ns, orders of magnitude faster than the theoretical limit for the twisted nematics.

This very fast optical response has many potential applications. In bit-addressed matrix display devices, for example, a threshold is necessary, and fast optical switching and bistable memory, or bistability of the optical states of each pixel, provide well-known advantages.¹⁶ Thus, a need for new liquid crystal materials with specially tuned properties is evident. The most interesting materials would possess the following properties: (1) A C* phase stable in a broad temperature range about room temperature; (2) high ferroelectric polarization density P ; (3) low orientation viscosity η ; and (4) orientability in the SSFLC cell. Additionally, the magnitude of the refractive index and dielectric constant anisotropies may need to be controlled.

Molecular Design Considerations

The fundamental requirement in FLC design is to obtain materials with tilted smectic liquid crystal phases. In general,

(15) (a) Handschy, M. A.; Clark, N. A. *App. Phys. Lett.* **1982**, *41*, 39. (b) Clark, N. A.; Handschy, M. A.; Lagerwall, S. T. *Mol. Cryst. Liq. Cryst.* **1983**, *94*, 213–234.

(16) For an interesting discussion of flat-panel displays in general and more detailed descriptions of two important non-liquid crystal approaches to the problem (electroluminescent and gas-plasma displays), see: Shuford, R. S. *Byte* **1985**, *10*, 130–136.

(13) Goodby, J. W.; Gray, G. W. *Smectic Liquid Crystals: Textures & Structures*; Blackie & Son: U.K., 1984.

(14) Clark, N. A.; Lagerwall, S. T. *App. Phys. Lett.* **1980**, *36*, 899.

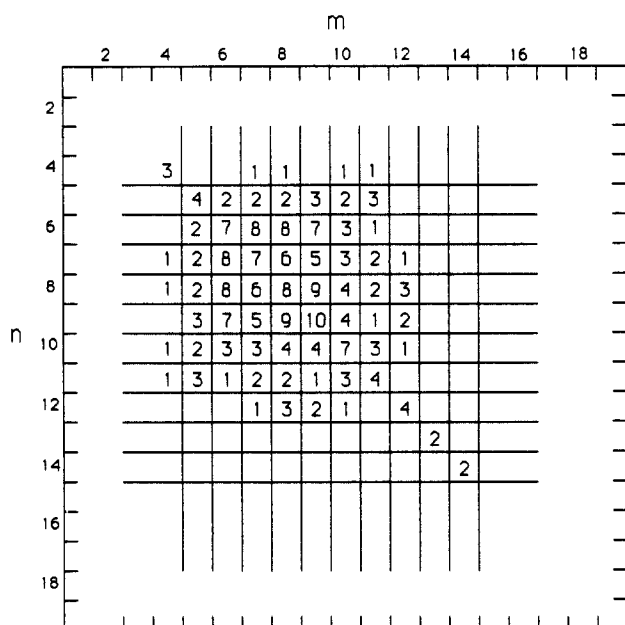


Figure 3. Relative occurrence of the smectic C phase in compounds of the general form: C_nH_{2n+1} -CORE- C_mH_{2m+1} , vs. n, m . Data are from ref 17 (about 300 compounds in all). Since core asymmetry is not recognized in this plot, it has been symmetrized about $n = m$. About 95% of these compounds have at least one alkoxy tail.

Table I. Ferroelectric Polarization of Some Known Smectic C* Materials

compound	P (nC/cm ²)	P (D/molecule) ^a
DOBAMBC (2)	-3	-0.009
HOBACPC (3)	-15	-0.04
DOBA-1-MBC (4)	40 ^b	0.11
MBRA (5)	-3	-0.008
6	<0.5	<0.0001
7, $n = 8, n' = 1$	-2.4	-0.006
7, $n = 10, n' = 1$	-1.8	-0.005
8	60 ^b	0.2
1, $R^1 = n$ -dodecyl, $R^2 = \text{ethyl}$	+14	+0.04
1, $R^1 = n$ -dodecyl, $R^2 = n$ -propyl	+14	+0.04

^a Effective dipole/molecule assuming density of 0.8 gm/cm³ for all materials. ^b Sign of P not reported.

liquid crystal phases appear in the phase diagram of rod-shaped molecules with a rigid core unit, as exemplified by the benzyldeneamino, phenylbenzoate, and biphenyl cores shown in the structures in Chart I and two "floppy" straight-chain hydrocarbon tails. Empirical data on known materials¹⁷ suggest that tilted smectic phases occur when the tails are of about equal length and of intermediate length (about seven carbons), and at least one tail is an alkoxy grouping (i.e., joined to the core via an oxygen atom). Figure 3 shows the occurrence of C phases as a function of tail length for a variety of compound classes in graphic form. The structures of several specific materials known to possess ferroelectric smectic C* phases are shown in Chart I.

In addition to obtaining a tilted smectic phase, one would also like to optimize the ferroelectric polarization and orientational viscosity. Specifically, in order to minimize the switching time in the SSFLC cell, materials with high polarization density and low orientational viscosity are required. Data concerning the polarization density for several of the materials shown in Chart I are known. Table I lists estimates of the maximum polarization

Table II. Phase Transition Temperatures for Compounds 1^a

R^2	R^1	n-nonyl	n-decyl	n-undecyl	n-dodecyl
Me		X $\xrightarrow{45}$ I 9 \xleftarrow{A} 38	X $\xrightarrow{40}$ A $\xrightarrow{51}$ I 30 \xleftarrow{A} 28 C* 7 \xleftarrow{A} 42	X $\xrightarrow{42}$ A $\xrightarrow{48.5}$ I	X $\xrightarrow{43}$ I 7 \xleftarrow{A} 42
Et		X $\xrightarrow{38}$ I 32 \xleftarrow{A} 38-35.5	X $\xrightarrow{36.7}$ A $\xrightarrow{39.4}$ I 27.8 \xleftarrow{A} 9 C* -4 \xleftarrow{A} 6	X $\xrightarrow{95}$ I	X $\xrightarrow{44}$ A $\xrightarrow{46.0}$ I 34.8 \xleftarrow{A} 27.6 C*
n-Pr		X $\xrightarrow{12}$ I	X $\xrightarrow{29}$ A $\xrightarrow{31}$ I 5 \xleftarrow{A} 30.7	X $\xrightarrow{28}$ A $\xrightarrow{32}$ I	X $\xrightarrow{35}$ A $\xrightarrow{42}$ I 37.5 \xleftarrow{A} 25 C* 5.7 \xleftarrow{A} 7

P observed for several compounds in Chart I in units of nC/cm².¹⁸ Given the density of the material in molecules/cm³, the polarization may be expressed in the more interesting form of Debye/molecule. While the densities of these compounds are not known, an estimate of P (Debye/molecule) assuming $D = 0.8$ gm/cm³ is given in the table. It is important to note however that comparisons of polarization densities shown in Table I must be made carefully, since the measurements were in general taken at different tilt angles θ . The best structure/ P comparisons would be between numbers taken at identical tilt angles. Also, the magnitude of the polarization in units of Debye/molecule gives the effective dipole moment per molecule contributing to P . The actual dipole moment per molecule contributing to P is attenuated by $1/\epsilon$, where ϵ is a dielectric constant for the medium (discussed in slightly more detail below). Thus, the actual dipole moment per molecule = the effective dipole per molecule $\cdot \epsilon$. Unfortunately, ϵ is not known for the materials listed in the table.

Even considering the above mentioned caveats, some interesting qualitative correlations do emerge from the numbers shown in Table I. Specifically, replacing the 2-methylbutyl chiral unit of DOBAMBC (2) by a 2-chloropropyl moiety, to give [(hexyloxy)benzylideneamino]-2-(chloropropyl)cinnamate (HOBACPC, 3), increases the polarization (effective dipole/molecule) by a factor of about 4.5. Replacement of the 2-methylbutyl tail unit of DOBAMBC by the isomeric 1-methylbutyl unit (DOBA-1-MBC, 4) increases the polarization by more than a factor of 10. These early observations have led to the conclusion that (1) a polar group attached to the stereogenic center may increase polarization and (2) movement of the stereogenic center close to the core may increase polarization.

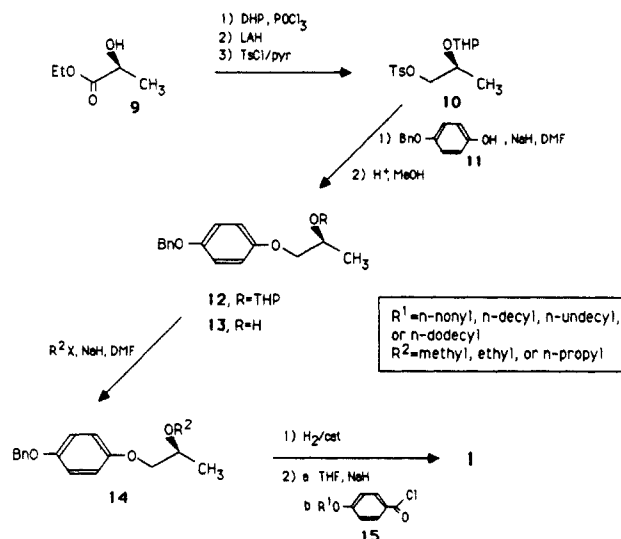
The latter supposition gains support from the work of the Chisso group, who has shown that compound 8, possessing the 1-methylheptyl chiral unit in combination with a commonly used LC core, exhibits the highest polarization of any material yet reported.¹⁸ In addition, observations of Goodby¹⁹ and the Chalmers group show that the polarization decreases as the stereogenic center of methyl-alkyl tails is moved further away from the core. For example, MORA-8 (6) was designed on the

(17) (a) Gray, G. W.; Goodby, J. W. *Mol. Cryst. Liq. Cryst.* **1976**, *37*, 157. (b) Gray, G. W.; Goodby, J. W. *Ibid.* **1978**, *48*, 127. (c) Demus, D.; Demus, H.; Zschke, H. *Flüssige Kristalle In Tabellen*; VEB Deutscher Verlag für Grundstoffindustrie; Leipzig, 1974. (d) Clark, N. A.; Lagerwall, S. T., personal communication.

(18) A major difficulty in the ferroelectric liquid crystal field has been a lack of consistent data on the sign and magnitude of the polarization for various compounds. The literature is replete with conflicting data on the magnitude of P for many compounds, and the sign of P is rarely given. To correct this unfortunate situation, Professor Lagerwall and his group at Chalmers Technical University have mounted a concerted effort to obtain consistent and accurate values for P for as many compounds as possible. Except for DOBA-1-MBC (4), all of the numbers given in Table I are a result of this effort and will be reported and discussed in detail elsewhere. We thank Professor Lagerwall for making them available to us prior to publication. The polarization of DOBA-1-MBC is presented in the following: Yoshino, K.; Ozaki, M.; Sakurai, T.; Sakamoto, K.; Honma, M. *Jpn. J. Appl. Phys., Part 2* **1984**, *23*, 175-177.

(19) Goodby, J. W.; Leslie, T. M. *Mol. Cryst. Liq. Cryst.* **1984**, *110*, 175-203.

Scheme I



assumption that increasing the length of the "floppy" connection between the stereogenic center and core would lower the melting point. Indeed, MORA-8 shows a C* phase in a very broad range of about room temperature (about 10–90 °C).²⁰ Its polarization however is so low it cannot be measured.

Our rationale for design of compounds 1 was based upon the following simple considerations. While a large effort on design of optimum core units has been expended in the liquid crystal field, relatively little work on exploration of novel chiral tail units for incorporation into ferroelectric liquid crystals has been reported. Thus, to our knowledge, outside the present work the compounds shown in Chart I indicate *all* of the chiral tail units incorporated into ferroelectric liquid crystals to date.²¹ In the first analysis, it was felt that the 2-alkoxy-1-propoxy chiral tail would prove useful for incorporation into smectic C forming molecules for the following reasons.

First, empirically the 2-alkoxy-1-propoxy unit conforms to the idea that a polar group be rigidly associated with the tetrahedral stereocenter of the tail. In addition, we conjectured that due to the well-known gauche effect²² molecular rigidity in the tail would be increased relative to a hydrocarbon tail, thereby leading to an increase in the strength of the molecular recognition processes responsible for the polarization of the phase.

Other important considerations were the following: (1) The phenylbenzoate core coupled with the diether tail is very chemically stable, and the phenylbenzoate core unit is known to promote formation of tilted smectic phases when coupled with simple achiral alkoxy tail units; (2) Added potential structural flexibility is gained due to the two readily varied *n*-alkyl chains in the tails. This was expected to allow for more tuning of the phase transition temperatures relative to compounds possessing only one readily varied alkyl tail; (3) The system is conveniently available synthetically from a simple starting material commercially available in enantiomerically enriched form—ethyl lactate; (4) The glycol diether units present were not expected to increase orientational viscosity relative to the simple alkoxy and halocarbon tails.

Results and Discussion

Synthesis. A simple approach to synthesis of compounds of type 1 has been developed, as outlined in the synthetic Scheme

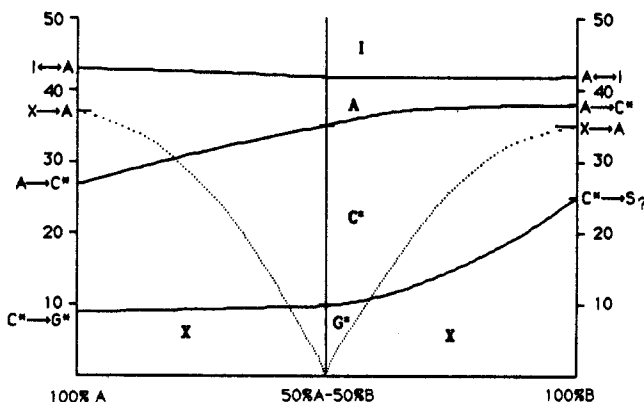


Figure 4. Phase diagram for the binary mixture of compound 1 R¹ = *n*-decyl, R² = ethyl (A) and R¹ = *n*-dodecyl, R² = *n*-propyl.

I. Ethyl L-(+)-lactate (ethyl (*S*)-2-hydroxypropanoate, 9) serves as enantiomerically enriched starting material. Conversion of (*S*)-ethyl lactate to the known nonracemic tetrahydropyranyl (THP) ether protected *p*-toluenesulfonate 10 is accomplished in a straightforward manner according to the procedure of Ghirardelli.²³ Alkylation of the known²⁴ monobenzyl ether of hydroquinone 11 with tosylate 10 under standard Williamson etherification conditions affords ether 12. Removal of the THP protecting group then gives the secondary alcohol 13 in good overall yield.²⁵

Starting with alcohol 13 a variety of chiral tail units of interest for incorporation into ferroelectric liquid crystal materials may be readily prepared. For the present purposes, simple methyl, ethyl, and *n*-propyl chains were appended by Williamson etherification, giving ethers 14. Removal of the benzyl ether protecting group by catalytic hydrogenation, then coupling of the resulting phenols with *p*-alkoxybenzoyl chlorides 15 (R = *n*-nonyl, *n*-decyl, *n*-undecyl, and *n*-dodecyl) affords the target liquid crystal compounds 1 (R¹ = *n*-nonyl, *n*-decyl, *n*-undecyl, *n*-dodecyl; R² = Me, Et, *n*-Pr).

Liquid Crystal Properties of Compounds 1. In fact, many of the expectations for compounds of type 1 are met in the actual materials synthesized. Phase behavior of the new compounds is shown in Table II. First, note that none of the materials possesses a thermodynamically stable C* phase. That is, upon heating of the crystalline solid, the compounds either melt directly to an isotropic liquid or enter a smectic A phase before becoming isotropic. Several compounds however exhibit super-cooled C* phases, as indicated in Table II in bold boxes. These phases appear reproducibly upon cooling of the isotropic liquid and may be stable for hours or even days, depending upon conditions. Such kinetically stable liquid crystal phases are very common and are termed *monotropic* phases.

Four of the new compounds exhibit monotropic C* phases below 30 °C. Interestingly, none of the compounds with a 9 or 11 carbon achiral tail shows a C* phase, while the C10 and C12 tail units seem to promote appearance of monotropic C* phases. This behavior represents yet another example of an odd–even effect, first observed in the hydrocarbon melting points and ubiquitous in liquid crystal chemistry.

It is quite possible to measure the optical rise time and ferroelectric polarization of materials with monotropic ferroelectric phases of the type exhibited by these compounds. Thus, for the purposes of developing structure–polarization relationships, the new materials are very interesting and useful. However, for device applications, and even for research with ferroelectric liquid crystals, C* phases thermodynamically stable at room temperature are required.

(20) Hallsby, A.; Nilsson, M.; Otterholm, B. *Mol. Cryst. Liq. Cryst.* **1982**, *82*, 61–68.

(21) Goodby, J. W. has explored the novel 2-chlorobutyrate and 2-trifluoromethyl units, but no smectic C* phases were observed.¹⁹ Solladie has reported some very interesting chiral LC's possessing nonracemic biphenylcyclohexylideneethanone cores. While smectic phases are observed, no tilted phases are reported: Solladie, G.; Zimmermann, R. *J. Org. Chem.* **1985**, *50*, 4062–4068.

(22) (a) Wolfe, S. *Acc. Chem. Res.* **1972**, *5*, 102. (b) Cowley, A. H.; Mitchell, D. J.; Whangbo, M.-H.; Wolfe, S. *J. Am. Chem. Soc.* **1979**, *101*, 5224.

(23) Ghirardelli, R. G. *J. Am. Chem. Soc.* **1973**, *95*, 4987–4990.

(24) Druey, J. *Bull. Chim. Soc. Fr.* **1935**, *2*, 1737–1741.

(25) Chiral shift studies using ¹H NMR at 250 MHz with the shift reagent tris[3-[(trifluoromethyl)hydroxymethylene]-*d*-camphorato] europium(III) proves that alcohol 13 is >95% enantiomerically pure, as expected.

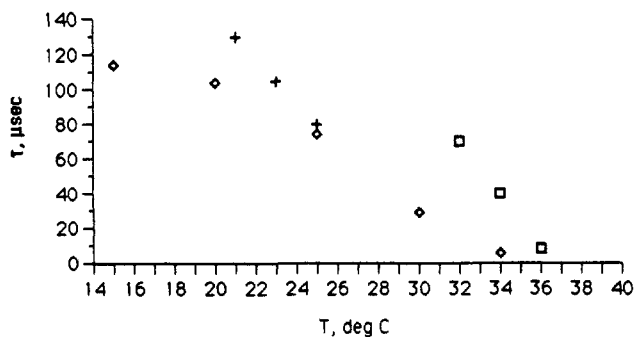


Figure 5. Optical rise time τ as a function of temperature at 15 V driving voltage for compound 1 $R^1 = n$ -dodecyl, $R^2 = n$ -propyl (\square), compound 1 $R^1 = n$ -decyl, $R^2 =$ ethyl (+), and the 50:50 mixture of these two compounds (\diamond). All measurements were made on 1 μ m thick samples shear-aligned between clean ITO (indium-tin oxide) coated glass plates viewed in transmission between crossed polarizers.

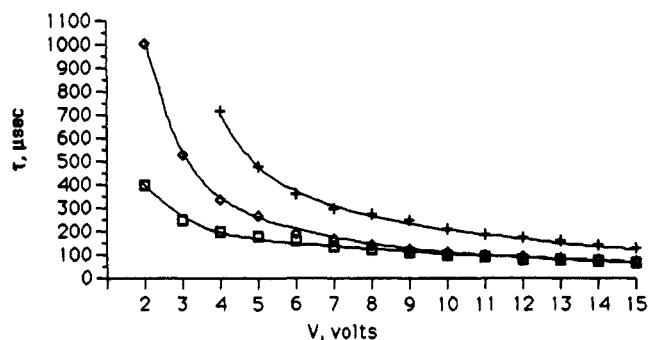


Figure 6. Optical rise times τ as a function of driving voltage for compound 1 $R^1 = n$ -dodecyl, $R^2 = n$ -propyl (\square , $T = 32.0$ °C), compound 1 $R^1 = n$ -decyl, $R^2 =$ ethyl (+, $T = 20.5$ °C), and the 50:50 mixture of these two compounds (\diamond , $T = 25.0$ °C). Measurements were made under conditions identical to those described for Figure 5.

It is common practice to broaden the temperature range of desired phases by formulating eutectic mixtures. Indeed, all commercial LC materials are multicomponent mixtures, in some cases containing seven or more individual compounds. This practice is effective since, for immiscible solids, melting point depression occurs upon mixing. However, in given liquid crystal phases (e.g., the A and C* phases) different compounds are in general miscible, and there is normally no depression observed in, for example, the A \leftrightarrow C* transition upon mixing. Thus, often the temperature range for the liquid crystal phases is broadened for mixtures. Even for pure compounds with monotropic phases, it is generally possible to obtain thermodynamically stable LC phases by formulation of mixtures.

In fact, many simple binary mixtures of compounds 1 with each other, and with members of other LC families, have been prepared.²⁶ For example, as shown in the phase diagram in Figure 4, a 50:50 mixture of compounds 1 ($R^1 = n$ -decyl, $R^2 =$ ethyl) and 1 ($R^1 = n$ -dodecyl, $R^2 = n$ -propyl) possesses a stable C* phase between 10 and 35 °C. Full characterization of these mixtures is in progress and will be reported in detail elsewhere. They are mentioned here to prove the utility of compounds 1 as ferroelectrics even though the pure compounds do not exhibit thermodynamically stable C* phases.

Electro-Optical Response and Polarization of Compounds 1. The electro-optic response times in the SSFLC geometry for compounds 1 ($R^1 = n$ -decyl, $R^2 =$ ethyl) and 1 ($R^1 = n$ -dodecyl, $R^2 = n$ -propyl) and for the 50:50 mixture of these compounds have been studied. Figure 5 shows the optical rise time τ as a function of temperature at 15 V driving voltage, and Figure 6 gives τ as a function of driving voltage for the same materials at several

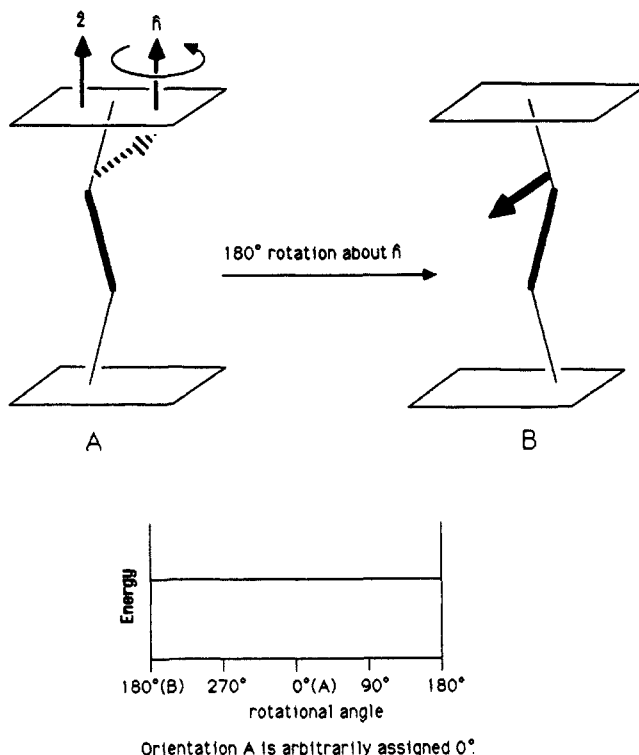


Figure 7. Single molecule in a smectic A phase.

temperatures close to room temperature. It should be noted that operationally, useful optical rise times in the SSFLC light valve of on the order of 100 μ s have been demonstrated at room temperature. Thus, while data on many compounds are lacking, pure compounds 1 ($R^1 = n$ -decyl, $R^2 =$ ethyl) and 1 ($R^1 = n$ -dodecyl, $R^2 = n$ -propyl) possess the fastest room temperature optical rise times τ reported to date. Also, the eutectic mixture illustrated in Figure 4 exhibits the fastest room-temperature switching time of any thermodynamically stable C* material yet reported.

The ferroelectric polarizations of compounds 1 ($R^1 = n$ -decyl, $R^2 =$ ethyl) and 1 ($R^1 = n$ -dodecyl, $R^2 = n$ -propyl) have also been measured, as shown in Table I.¹⁸ Note that as expected, the polarization density of the lactic ethers is, in fact, substantially enhanced relative to compounds 7, which possess very similar structures but without benefit of the glycoldiether unit.

A Simple Model for the Origin of P in Ferroelectric Liquid Crystals

The Diastereomeric Relationships Responsible for the Ferroelectric Polarization. In order to interpret the polarizations exhibited by FLC's and to design in a directed way new materials with increased polarization densities, it is necessary to understand the molecular level origin of the polarization P exhibited by C* materials. Meyer's symmetry arguments predicting the existence of the polarization must be applied at the molecular structural level.²⁷ In host-guest chemistry in solution, it is conceptually easy to see how molecular recognition can occur. For example, the complexes formed between an enantiomerically pure host and two enantiomers of a chiral guest are diastereomeric. That the equilibrium formation constant for the complexes may differ in magnitude follows directly. What are the diastereomeric relationships leading to the ferroelectric polarization?

Some insight into this question can be achieved by consideration of the crude models shown in Figures 7 and 8. Here, a chiral liquid crystal molecule is represented by the zigzag figure, intended to illustrate the core and tail units, with an arrow rigidly placed on one of the tails normal to the plane of the zigzag, affording a chiral construction. Suppose for the present purpose that only one rigid conformation of the "molecule" is possible. Figure 7A

(26) Some properties of the mixture composed of 1 ($R^1 = n$ -decyl, $R^2 =$ ethyl) and 7 ($n=10$, $n'=3$) have been reported: Lagerwall, S. T.; Wahl, J.; Clark, N. A. Proceedings of the 1985 International Display Research Conference in San Diego, October 1985, pp 213-221.

(27) Meyer, R. B. *Mol. Cryst. Liq. Cryst.* 1977, 40, 33.

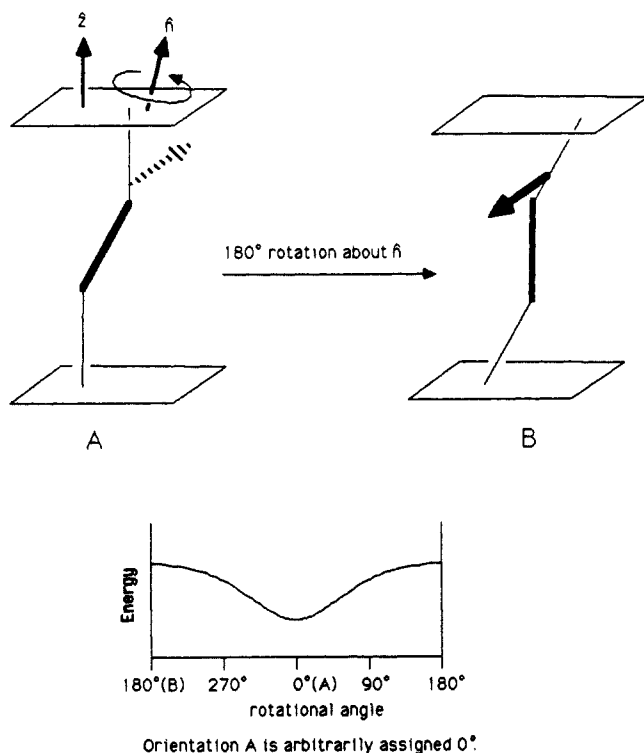


Figure 8. Single molecule in a smectic C phase.

represents a single molecule in a smectic A phase (similar to the smectic C, but *untilted*, that is \hat{z} and \hat{n} are parallel). The smectic planes of the phase are represented by the rectangular constructions in the figure.

Consider the supermolecular system which includes the molecule and the smectic planes. A rigid rotation through some angle (in this case 180°) of the molecule about \hat{n} produces the new "rotational state" B, as shown in Figure 7. Note that the "rotational states" A and B, including the smectic planes, are *homomeric* (superimposable by rigid translation) and will have equal energy. Indeed, all rotational states of the molecule in the smectic A phase on average will have equal energy, as indicated in the energy diagram showing potential energy as a function of rotational angle. Rotation of molecules about the director in a smectic A phase has no barrier on average, and the rate of the process is determined by a "rotational viscosity" or rotational diffusion coefficient.

Now consider the analogous states in a smectic C phase, as shown in Figure 8. Here, including the smectic planes, the states A and B (in Figure 8) are *diastereomeric* (not rigidly superimposable and not mirror images) and will in general differ in energy. Indeed, in a chiral or achiral smectic C phase any rigid rotation of a single molecule about \hat{n} leads to a diastereomeric "state". On the time average or averaging over an ensemble of molecules, this rotation is an activated process, in the sense that there is a barrier in the energy surface for the rotation, and the rate for the process is determined by the depth and shape of the energy surface. In general, one rotational state will be preferred—that existing at the bottom of the rotational energy well.

Suppose the orientation shown in Figure 8A (arbitrarily assigned rotation angle 0° in the diagram) was preferred. If the arrow represented a molecular dipole (drawn from $-$ to $+$), then an aggregate of such molecules would possess a positive ferroelectric polarization. The magnitude of the polarization would depend upon the magnitude of the dipole for each molecule and upon the depth and shape of the energy well orienting the molecules. Note that if the molecules were achiral (no arrow) or an aggregate of such molecules were racemic, then even though the molecules are rotationally ordered, no net polarization would result.

Of course, the smectic planes in a real phase are not present as physical objects. Also, many conformations are possible for the molecules in the phase. We suggest that one productive way

to more realistically consider the problem is as follows. The molecules are ordered with respect to *rotational and conformational states* by a "surface of constant molecular mean field" or time-average van der Waals surface resulting from interactions with neighboring molecules in the aggregate. This surface may be considered a type of *binding site*, quite analogous to that present in organic and biological host molecules. In a smectic A phase or any untilted phase, this binding site will have cylindrical symmetry. We suggest that in a tilted phase such as the smectic C, the cylindrically symmetrical binding site does not simply tilt over, but the symmetry of the binding site changes. In the smectic C phase, while the binding site must possess a C_2 axis along the two-fold symmetry axis of the phase,¹¹ there is no longer a mirror plane normal to the director. This change in symmetry of the time average binding site in a tilted phase is ultimately responsible for the ferroelectric polarization.

An Expression for P in Terms of Molecular Dipoles. Given the above arguments, how can we write the ferroelectric polarization in terms of individual molecular dipoles? First, it is necessary to extend our molecular model from a rigid zigzag shape with an arrow representing a dipole, to more realistic constructions, for example, Dreiding framework models or CPK spacefilling models, with conformational flexibility. Ultimately, it may be more useful to consider molecular mechanics constructions combined with monte-carlo statistical dynamics calculations or some other more sophisticated model. For the present however consider the origins of P in terms of framework or spacefilling models for the molecules.

Suppose we are given or assume a binding site shape. Two factors must be considered: (1) the conformations are oriented by the binding site with respect to the *tilt plane* (the plane containing \hat{z} and \hat{n}) and *tilt direction*. We find it useful to separate these two factors by considering the contribution to the polarization of each conformation, then summing over all conformations present. Physically, this is equivalent to microscopic examination of the phase on a very short time scale, where conformational changes are slow. The polarization may thus be written as

$$P = \sum D_i P_i \quad (2)$$

over all i conformations

where D_i is the number density for the i th conformation, and P_i is the ensemble average contribution to the polarization for that conformation.

In order to discuss how each conformation is ordered by the binding site, some geometry must be set down. Firstly, it should be pointed out that macroscopically the director \hat{n} is defined in several different ways (optical properties of the phase, X-ray patterns), but on a molecular level, the director (and tilt angle) is not really well-defined. The director \hat{n} is usually considered as some average long axis of the molecule, but exactly where the director lies relative to a specific conformation in the phase is not rigorously defined, and indeed may depend upon the experiment used to measure it. For example, the optical axis of the phase depends upon the axis of maximum high frequency polarizability of the molecules, while the director defined by X-ray diffraction depends upon the electron density distribution.²⁸ For the present purposes, the director may simply be considered as the axis of minimum rotational inertia for each conformation.

Given the director \hat{n} for a conformation, the smectic C tilt plane is simply the plane containing both \hat{z} and \hat{n} . To establish the orientation of conformations in the C^* binding site, we define the *molecular tilt plane* for a conformation as the plane parallel to the smectic C tilt plane bisecting the *preferred rotational state* of the conformation in the binding site. That is, each conformation will be rotationally ordered in the C^* phase, just as the zigzag model is rotationally ordered in Figure 8. In general, one rotational state will be preferred or will lie at the bottom of a rotational potential energy well. The molecular tilt plane simply defines how

(28) Bartolino, R.; Doucet, J.; Durand, G. *Ann. Phys. (Paris)* **1978**, *3*, 389–396.

the conformation in the preferred rotational state is oriented in the phase relative to the tilt plane.

We can now express P in terms of molecular dipoles as follows. The contribution to the polarization density for each conformation is dissected into three terms: (1) μ_{\perp} —the component of molecular electric dipole moment *normal to the molecular tilt plane* for a given conformation; (2) the ROF—a scalar quantity (unitless, $0 \leq \text{ROF} \leq 1$) which we term the rotational orientation factor, reflecting the strength of the effect giving rise to rotational orientation of molecules the conformation (this is related to the depth and shape of the energy well orienting the conformation, or equivalently, to the shape and "hardness" of the binding site); and (3) ϵ —a dielectric constant of the medium defined by the following equation: $P = (Dp)/\epsilon$, where P is the observed bulk polarization density, D is the number density of molecules, and p is the average molecular dipole moment in the direction $(\hat{z} \times \hat{n})$. A reasonable estimate of ϵ is simply the mean dielectric constant of the medium.

At this point two cases, differentiated by the symmetry of the binding site, must be considered. For an achiral C phase the binding site and rotational energy surface have mirror symmetry about the tilt plane. In a chiral, nonracemic C phase however the binding site and energy surface, in general, are dissymmetric. For the present, we will focus on the case where the rotational energy surface and binding site are symmetrical about the tilt plane. For a ferroelectric phase, this would correspond to the situation occurring when an achiral C phase is doped with a small amount of enantiomerically pure liquid crystal material. Such phases are well-known to be ferroelectric.

If the binding site and rotational energy surface possess a mirror plane congruent with the tilt plane, then the contribution to the polarization density for a single conformation i may be written as $P_i = \mu_{\perp i} \text{ROF}_i / \epsilon$, and

$$P = \sum D_i \mu_{\perp i} \text{ROF}_i / \epsilon \quad (3)$$

over all i conformations

If the binding site does not possess mirror symmetry about the tilt plane, then a more complex expression for P is required, which will not be discussed here. It is easy to demonstrate however that eq 3 fails for a chiral binding site. For example, suppose μ_{\perp} is zero, but μ_{\parallel} , the component of the molecular dipole parallel to the molecular tilt plane, is not zero. If the binding site has reflection symmetry about the tilt plane, P would be zero according to eq 3. But, if the binding site (and energy well orienting the rotational states of the molecules) is dissymmetric about the tilt plane, P will be nonzero in this case, and eq 3 fails.

Speculation Concerning the Shape of the C* Binding Site for Simple Alkoxyphenyl Alkoxybenzoates. Exactly how the symmetry of the binding site in a C phase is imposed and the shape of the binding site are fundamental questions. In considering the question of the actual shape of the binding site for specific materials, one must know or guess at the preferred conformation of the tail units in the C phase. In fact, there is a considerable body of experimental evidence²⁹ suggesting that in liquid crystal molecules the predominate conformation for alkyl tails is all anti, with the probability of gauche bends in the chains being small at bonds near the core and increasing with distance from the core.

In a tilted phase, intuition and examination of CPK molecular models suggest that *the tail units should be less tilted than the cores*, and experimental evidence corroborates this interpretation.^{28,30} Thus, we suggest an average zigzag conformation for the molecules, with a preferred rotational orientation as indicated in Figure 8A, is close to the truth.

For an achiral or racemic smectic C the binding site maintaining this conformation and orientation would have the symmetry of

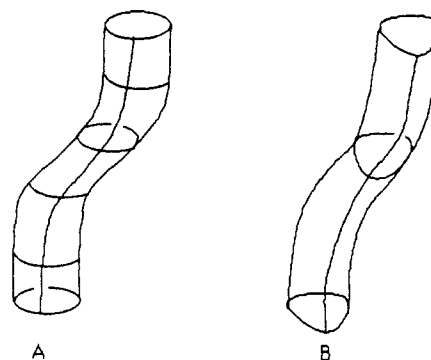


Figure 9. Two possible shapes for the "binding site" in smectic C phases.

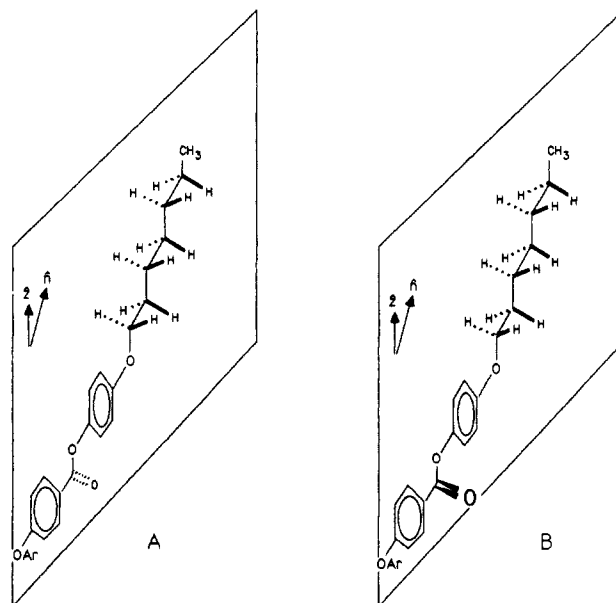


Figure 10. A possible preferred orientation of a simple *p*-alkoxy phenylbenzoate in the C phase, showing the smectic tilt plane (congruent with the molecular tilt plane in this case).

a *bent cylinder*, as illustrated in Figure 9A. In a chiral, nonracemic smectic C phase, the binding site must lose the mirror symmetry of Figure 9A (a σ plane parallel to the plane of the paper) to take a shape with less symmetry, for example, that shown in Figure 9B.

While there is currently not enough data to allow even an educated guess concerning how alkoxyphenyl alkoxybenzoates such as compounds 1 or 7 are actually oriented by their respective C* binding sites or to propose a molecular-level model for their ferroelectric polarization, it seems reasonable to at least consider the problem in terms of the model proposed herein in order to illustrate how it might be used.

Consider first a simple achiral phenyl benzoate with *n*-alkoxy tails. In the simplest model, in the smectic C phase the tails are fully extended in an all anti conformation, such that in the preferred rotational state (1) all of the carbon atoms of the tail are in the tilt plane and (2) the tails are bending away from the tilt direction (i.e., the tails are less tilted than the core). Figure 10A illustrates a (*p*-heptyloxy)phenyl benzoate molecule oriented in this manner and shows the molecular tilt plane (congruent with the smectic C tilt plane for the preferred rotational state) for the conformation.

An important concept, that of *conformational averaging* of molecular dipoles, is conveniently illustrated here. Thus, for the conformation shown in Figure 10A, the phenyl benzoate ester unit contributes to a dipole moment normal to the tilt plane— μ_{\perp} (it is well-known that in phenyl benzoates, the carbonyl grouping is tilted away from the plane of the phenyl ring). Since the molecules are oriented rotationally (ROF \neq 0), this conformation will contribute to a polarization P of the phase ($P_{10A} =$

(29) (a) Dong, R.; Samulski, E. T. *Mol. Cryst. Liq. Cryst.* **1982**, *82*, 73–79. (b) Samulski, E. T.; Dong, R. *J. Chem. Phys.* **1982**, *77*, 5090–5096. (c) Hirokazu, T.; Samulski, E. T. *Mol. Cryst. Liq. Cryst.* **1983**, *101*, 163–173. (d) Samulski, E. T. *Isr. J. Chem.* **1983**, *23*, 329–339. (e) Hirokazu, T.; Samulski, E. T. *Liq. Cryst. Ordered Fluids* **1984**, *4*, 597–613. (30) (a) Paranjpe, A. S. *Mol. Cryst. Liq. Cryst.* **1982**, *82*, 93–98. (b) Bryan, R. F.; Leadbetter, A. J.; Mehta, A. I.; Tucker, P. A. *Mol. Cryst. Liq. Cryst.* **1984**, *104*, 257–264.

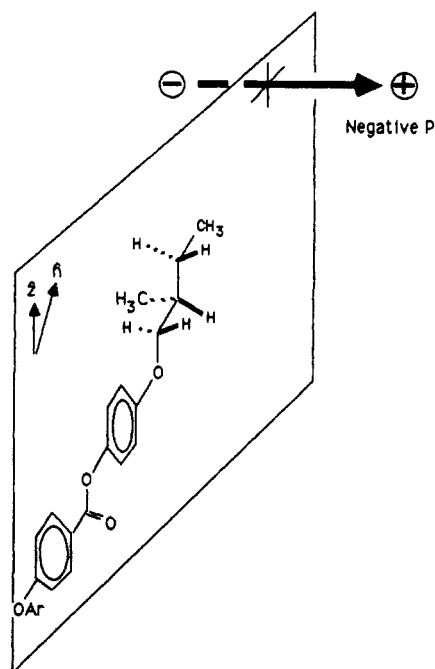


Figure 11. A *p*-(*S*)-2-(((methylbutyl)oxy)phenyl) benzoate **7** oriented with the butyl chain in the smectic tilt plane. The experimentally determined sign of the polarization is indicated by the *P* vector in the drawing.

$\mu_{\perp 10A} \text{ROF}_{10A} / \epsilon$). However, the material is not chiral, and an aggregate of such molecules would possess no spontaneous polarization. This is due to the fact that an equal number density of molecules will exist in the conformation illustrated in Figure 10B, wherein the orientation of the ester unit leads to an equal magnitude but opposite sign for μ_{\perp} . Since the ROF for conformation 10B is equal to that for 10A, the contributions of these conformations to *P* averages exactly to zero. This is also true for all other conformations with a dipole moment normal to the tilt plane.

Now consider the case where a chiral (*S*)-2-methylbutyl unit replaces one of the achiral alkoxy tails of the phenyl benzoate (compounds **7** with *n* = 1). In a first-order model, consider only the conformation wherein the longest chain of the alkyl tails is anti, as shown in Figure 11. While there is now no way to establish how the tilt plane cuts this conformation in the *C** phase, we propose that any contribution to a ferroelectric polarization from the ester unit in the core will be zero by the same argument utilized for the achiral case above. However, there will be a

nonzero μ_{\perp} which is *not* averaged to zero by conformational changes, deriving from the arrangement of molecular dipoles on the chiral tail. This will lead to the observed net spontaneous polarization for the compound. Note that the actual experimentally determined ferroelectric dipole direction for compounds **7** with *n* = 1 is indicated in the figure.

Unfortunately, at this point there is no experimental evidence allowing an estimate of the conformations present in the phase nor of which molecular dipoles are contributing to *P*. It is important however to note that for compound **7**, *P* is relatively small (−0.005 D/molecule). Even assuming an ϵ of 10 (probably an upper limit), the average molecular dipole contributing to *P* is only about 0.05 Debye.

When the 2-methylbutyl chiral tail is replaced by the 2-alkoxypropyl unit of compounds **1**, the polarization density increases by about a factor of 8 relative to compounds **7**, and the polarization is positive for both **1** (R^1 = *n*-decyl, R^2 = ethyl) and **1** (R^1 = *n*-dodecyl, R^2 = *n*-propyl), *P* = +0.04 Debye/molecule). Figure 12 shows three likely conformations for the (*S*)-2-alkoxypropoxy tail oriented similarly to the orientations shown for Figures 10 and 11. The dipole direction measured experimentally (positive *P*) is also indicated in the figure. Note that this model is very approximate, since the tilt plane in conformations A and B (in Figure 12) would cut the conformations at a point biased toward the longest portion of the tail. A detailed interpretation of the observed polarizations is again not possible since in this system it is not known what conformations are present in the *C** phase or which bond dipoles contribute to the polarization.

Clearly, we are just scratching the surface with regard to an understanding of the molecular level origins of the ferroelectric polarization of *C** phases. Even given ϵ , the conformations present in the phase, and the molecular tilt plane for each conformation, the polarization still could not be calculated since the actual binding site in a chiral, nonracemic phase is less symmetrical than the simple bent cylinder. For such a binding site, eq 3 is no longer valid. It is possible that dissymmetry in the binding site may prove an important factor. Indeed, this concept is particularly interesting, since it involves a very novel form of *chiral recognition* occurring in the liquid crystal phase. It should be possible to probe this form of chiral recognition by careful measurement of *P* as a function of enantiomeric purity of the material in the phase.

Even given the low level of detailed understanding of the origins of *P* in ferroelectric liquid crystals, the very simple models discussed above suggest many possible targets for synthesis which should possess *enhanced polarization density* and *predictable sign of the polarization*. Once *C** compounds are prepared wherein the bond dipoles contributing to *P* are unambiguous and have known values, studies on the conformational surface of the molecules in the phase and measurement of ϵ should lead to a

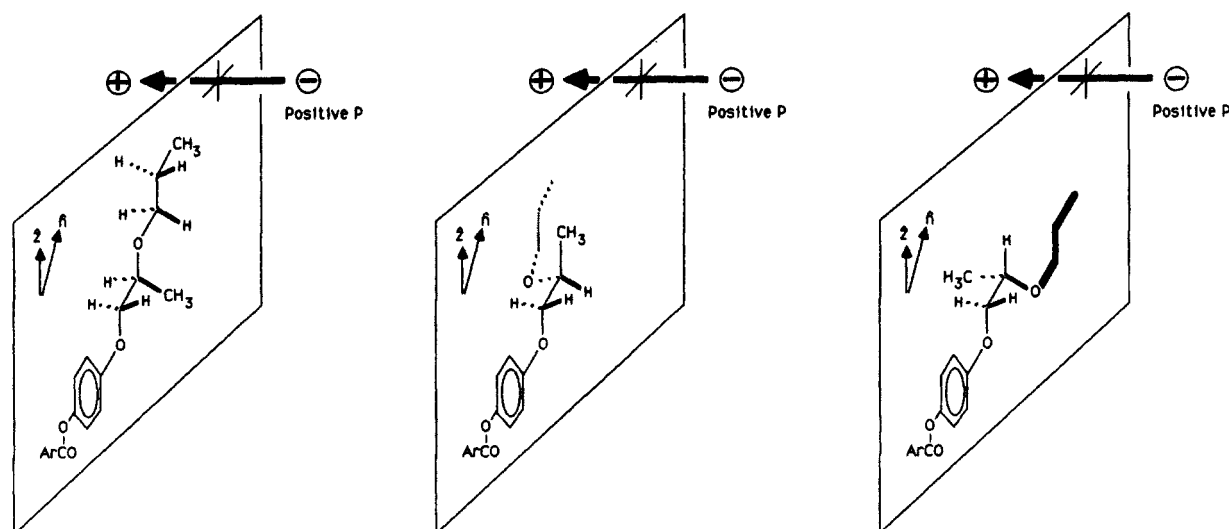


Figure 12. Three possible conformations of compound **1** R^2 = *n*-propyl. The experimentally determined sign of the polarization is indicated on each drawing.

better understanding of the rotational orientation and dynamics of the molecules in the phase.

Finally, we point out that the "binding site" model itself is in a way quite contrived and is suggested as a potentially powerful way to think about the problem of design of new materials. In a sense, however, the molecular recognition processes occurring in liquids is richer and more complex than that occurring upon complexation of a guest by a relatively rigid host. Considered in another way, synthesis of a new ferroelectric liquid crystals and measurement of their polarizations actually provides a very sensitive and novel probe of molecular dynamics occurring in liquid crystal phases, adding an extra dimension to the problem and providing a potential wealth of information concerning properties of liquids which would be very difficult to obtain otherwise.

Conclusion

A new class of ferroelectric liquid crystal materials has been prepared. Although the ferroelectric phases are monotropic, the new compounds possess useful properties for incorporation into SSFLC light valves, including the fastest room temperature electro-optical switching times of any known pure FLC's. Utilizing these compounds, a binary eutectic mixture has been formulated possessing a stable room temperature FLC phase with the fastest electro-optical switching times of any known FLC mixtures. Also, a simple model for the ferroelectric polarization of tilted nonracemic liquid crystal phases is proposed. It is suggested that the polarization can be productively considered in terms of molecular recognition occurring in the FLC phase, where the individual molecules are oriented by a "C*" binding site with the shape, roughly, of a bent cylinder.

Experimental Section

All ^1H NMR spectra were recorded at 250 MHz on a Bruker WM-250 instrument unless otherwise indicated. ^1H NMR spectra taken at 90 MHz were recorded on a Varian EM-390 spectrometer. ^{13}C NMR spectra were recorded on the Bruker WM-250 instrument at 69.2 MHz. Infrared spectra were recorded with a Perkin-Elmer 727B IR spectrometer, and mass spectra were taken on a JEOL MAT CH5 instrument. Analytical thin-layer chromatography (TLC) was performed on glass silical gel plates (0.25 mm thick E. Merck silica gel 60-F254), and chromatographic purifications were performed by using flash chromatography on E. Merck 40-63 μ normal phase silica gel.

Normal melting points obtained in the course of the synthetic work were taken on a Fisher-Johns melting point apparatus and are uncorrected. Phase transition data was obtained utilizing a hot stage polarizing microscope. The temperature of the stage was controlled and monitored with an Instec mK1 temperature controller running off an Apple 2e computer.³¹ Optical response times were measured on 1 μm thick SSFLC light valves with shear-aligned C* phases between smooth, clean ITO plates. A step voltage was applied, and the intensity of the transmitted light from a He-Ne laser passing through the SSFLC light valve between crossed polarizers was measured as a function of time with a fast photodiode.

"Dry" solvents were dried immediately prior to use. Ether and tetrahydrofuran (THF) were distilled from purple solutions of benzophenone and sodium; pyridine and pentane were distilled from calcium hydride; dimethylformamide (DMF) was distilled at reduced pressure and then stored for 3 days over 3-Å molecular sieves prior to use. Ethyl L-(+)-lactate (ethyl (S)-2-hydroxypropanoate), obtained from Aldrich Chemical Co., was purified by distillation and stored over 3-Å sieves. *p*-Alkoxybenzoic acids, obtained from Frinton Laboratories, were purified by recrystallization from ethanol prior to use. The corresponding acid chlorides were prepared by treatment of the acids with Aldrich Gold Label oxalyl chloride in benzene. (*p*-Benzoyloxy)phenol (monobenzene) was prepared by the method of Druey²⁴ or purchased from Eastman Kodak Company and recrystallized from ethanol.

Combustion analyses were performed by Galbraith Laboratories, Knoxville, TN.

1-(Benzoyloxy)-4-[(S)-2-[(tetrahydro-2-pyranyloxy]propoxy]benzene (12). To an argon-flushed flask containing 0.6 g (25.4 mmol) of oil-free sodium hydride was added 100 mL of dry DMF and 3.8 g (19 mmol) of (*p*-benzyloxy)phenol (11). The resulting mixture was allowed to stir for 15 min before a solution of 4.0 g (12.7 mmol) of tosylate 10²³ in 50 mL of DMF was added. The progress of the reaction was followed by TLC

(product R_f 0.58 with 4:1 ethyl acetate/hexanes as eluting solvent). When the reaction was judged complete (≈ 8 h), solvent was removed by rotary evaporation in vacuo, and excess sodium hydride was carefully quenched by addition of water. The resulting aqueous mixture was extracted with diethyl ether, and the organic phase was dried over anhydrous magnesium sulfate. Filtration and removal of solvent by rotary evaporation gave crude product which was purified by flash chromatography on silica gel eluting with 85:15 hexanes/ethyl acetate, affording 3.7 g (85%) of triether 12 as a mixture of diastereomers. Crystallization from ethanol/water gives material with mp 68.8–69.5 °C: ^1H NMR (CDCl_3) δ 1.25 and 1.30 (two doublets, 3 H, $J = 6.6$ Hz, RCH_3), 1.6 (m, 6 H, THP), 3.50 (m, 2 H, THP OCH_2CH_2), 3.83–4.15 (m, 3 H, $\text{ROCH}_2\text{CH}[\text{CH}_3]\text{OR}$), 4.85 (m, 1 H, THP acetal H), 4.99 (s, 2 H, ArCH_2O), 6.89 (m 4 H, Ar H), 7.4 (m, 5 H, Ar H); ^{13}C NMR (CDCl_3) δ 16.81, 18.56, 19.45, 19.74, 25.53, 30.98, 31.02, 62.15, 62.60, 70.44, 70.89, 71.52, 72.67, 72.88, 96.60, 98.87, 115.73, 115.76, 116.01, 116.03, 127.36, 127.75, 128.45, 137.47, 137.51, 153.25, 153.54, 153.62; IR (CHCl_3) 3000, 2920, 1500, 1380, 1220, 1030, 1000, 825 cm^{-1} ; mass spectrum, m/z (rel intensity) 342 (P^+ , 25), 90 (100), 84 (79). Anal. Calcd for $\text{C}_{21}\text{H}_{26}\text{O}_4$: C, 73.66; H, 7.68. Found: C, 73.55; H, 7.52.

1-(Benzoyloxy)-4-[(S)-2-hydroxypropoxy]benzene (13). To a flask containing 0.1 g of amberlite (Malinkrodt) sulfonic acid ion exchange resin suspended in 50 mL of methanol was added a solution of 1.05 g (3.07 mmol) of THP ether 12 in 20 mL of methanol. The resulting stirred reaction mixture was heated to 45 °C (oil bath). After 3.5 h, the reaction mixture was allowed to cool and filtered, and volatiles were removed by rotary evaporation, affording crude product which is quite clean as judged by TLC and ^1H NMR. This material may be purified by flash chromatography on silica gel, affording 785 mg (98%) of alcohol 13 as a white solid (mp 94.8–95.3 °C): ^1H NMR (90 MHz, CDCl_3) δ 1.29 (d, 3 H, $J = 6.3$ Hz, R-CH_3), 2.20 (s, 1 H, OH), 3.84 (m, 3 H, (m, 3 H, $\text{R-OCH}_2\text{CH}[\text{CH}_3]\text{OR}$)), 5.04 (s, 2 H, ArCH_2O), 6.93 (s, 4 H, Ar H), 7.35 (s, 5 H, Ar H); ^{13}C NMR (CDCl_3) δ 18.77, 66.31, 70.82, 74.24, 115.72, 116.04, 127.39, 127.82, 128.49, 137.34, 153.10, 153.44; IR (CDCl_3) 3275 (OH) 2900, 1500, 1220, 1010, 820; mass spectrum, m/z (rel intensity) 258 (P^+ , 64), 90 (100). Anal. Calcd for $\text{C}_{16}\text{H}_{18}\text{O}_3$: C, 74.40; H, 7.02. Found: C, 74.30; H, 7.05.

Representative Procedure for Alkylation of Alcohol 13. **1-(Benzoyloxy)-4-[(S)-2-ethoxypropoxy]benzene (14, $\text{R}^2 = \text{Ethyl}$).** To an argon-flushed flask containing 300 mg (12.5 mmol) of oil-free sodium hydride was added 60 mL of dry DMF followed by a solution of 2.15 g (8.3 mmol) of alcohol 13 in 25 mL of DMF. After stirring for an additional 15 min, 1.75 g (0.90 mL, 11.25 mmol) of neat ethyl iodide was added to the reaction mixture. After 8 h, the reaction was worked up as for synthesis of ether 12 to give crude product which was purified by flash chromatography on silica gel eluting with 9:1 hexanes/ethyl acetate, ($R_f = 0.38$) affording 2.14 g (90%) of ether 14 ($\text{R}^2 = \text{ethyl}$) as a white solid (mp 35.5–36.0 °C): ^1H NMR (CDCl_3) δ 1.20 (m, 6 H, R-CH_3), 3.60 (m, 2 H, $\text{O-CH}_2\text{CH}_3$), 3.84 (m, 3 H, (m, 3 H, $\text{R-OCH}_2\text{CH}[\text{CH}_3]\text{OR}$)), 5.00 (s, 2 H, ArCH_2O), 6.86 (m, 4 H, Ar H), 7.40 (m, 5 H, Ar H); ^{13}C NMR (CDCl_3) δ 15.57, 17.45, 64.59, 70.89, 72.69, 73.65, 115.75, 116.03, 127.37, 127.76, 128.46, 137.49, 153.25, 153.56; IR (CDCl_3) 2960, 2900, 1600, 1495, 1380, 1220, 1040, 740 cm^{-1} ; mass spectrum, m/z (rel intensity) 287 ($\text{P}^+ + 1$, 38), 286 (P^+ , 85), 90 (100). Anal. Calcd for $\text{C}_{18}\text{H}_{22}\text{O}_3$: C, 75.50; H, 7.74. Found: C, 77.73; H, 7.82.

Analytical Data for Compounds 14 ($\text{R}^2 = \text{Methyl}$ and $\text{R}^2 = n\text{-Propyl}$) Follow. **1-(Benzoyloxy)-4-[(S)-2-methoxypropoxy]benzene (14, $\text{R}^2 = \text{Methyl}$):** white solid (mp 57–58.5 °C): ^1H NMR (90 MHz, CDCl_3) δ 1.25 (d, 3 H, $J = 6.2$ Hz, R-CH_3), 3.42 (s, 3 H, OCH_3), 3.83 (m, 3 H, $\text{R-OCH}_2\text{CH}[\text{CH}_3]\text{OR}$), 4.98 (s, 2 H, ArCH_2O), 6.90 (s, 4 H, Ar H), 7.40 (br s, 5 H, Ar H); ^{13}C NMR (CDCl_3) δ 16.59, 56.78, 70.80, 72.29, 75.36, 115.69, 115.95, 127.35, 127.74, 128.43, 137.41, 153.23, 153.42; IR (CDCl_3) 3025, 2950, 2880, 1600, 1520, 1464, 1390, 1240, 1120, 1048, 840 cm^{-1} ; mass spectrum m/z (rel intensity) 272 (P^+ , 48), 90 (100). Anal. Calcd for $\text{C}_{17}\text{H}_{20}\text{O}_3$: C, 74.97; H, 7.40. Found: C, 75.03; H, 7.32.

1-(Benzoyloxy)-4-[(S)-2-propoxypropoxy]benzene (14; $\text{R}^2 = n\text{-Propyl}$): colorless liquid; ^1H NMR (90 MHz, CDCl_3) δ 0.89 (t, 3 H, $J = 6.3$ Hz, $\text{OCH}_2\text{CH}_2\text{CH}_3$), 1.28 (m, 5 H, $\text{R-OCH}_2\text{CH}[\text{CH}_3]\text{OR}$) and $\text{OCH}_2\text{CH}_2\text{CH}_3$), 3.49 (m, 2 H, $\text{OCH}_2\text{CH}_2\text{CH}_3$), 3.85 (m, 3 H, (m, 3 H, $\text{R-OCH}_2\text{CH}[\text{CH}_3]\text{OR}$)), 4.99 (s, 2 H, ArCH_2O), 6.90 (m, 4 H, Ar H), 7.40 (m, 5 H, Ar H); IR (CHCl_3) 2950, 2880, 1520, 1464, 1390, 1240, 1040, 840 cm^{-1} ; mass spectrum, m/z (rel intensity) 301 ($\text{P}^+ + 1$, 48), 300 (P^+ , 68), 90 (100). Anal. Calcd for $\text{C}_{19}\text{H}_{24}\text{O}_3$: C, 75.97; H, 8.05. Found: C, 76.20; H, 8.13.

Representative Procedure for Debenzylation of Ethers 14, *p*-[(S)-2-Ethoxypropoxy]phenol. A flask fitted with a gas inlet tube was charged with a suspension of 10% palladium on carbon (0.425 g) in 10 mL of ethanol. Hydrogen was allowed to bubble through the stirred suspension for 30 min before a solution of 0.425 g (1.49 mmol) of benzyl ether 14 ($\text{R}^2 = \text{ethyl}$) in 10 mL of ethanol was added. After the reaction was

(31) Instec, Inc., P.O. Box 7246, Boulder, CO 80306.

judged complete by TLC (about 8 h, product R_f 0.28 eluting with 3:2 hexanes/ethyl acetate) hydrogen ebullition was stopped, and the resulting suspension was filtered through a Celite pad. The filtrate was concentrated by rotary evaporation, and the resulting crude product was purified by flash chromatography on silica gel to give 0.262 g (90%) of *p*-[(*S*)-2-ethoxypropoxy]phenol as a white solid (mp 83–83.5 °C): ^1H NMR (90 MHz, CDCl_3) δ 1.20 (m, 6 H, ROCH_2CH_3 and $\text{ROCH}_2\text{CH}(\text{CH}_3)\text{OR}$), 3.60 (m, 2 H, ROCH_2CH_3), 3.80 (m, 3 H, (m, 3 H, $\text{ROCH}_2\text{CH}(\text{CH}_3)\text{OR}$)), 5.22 (s, 1 H, ArOH), 6.75 (s, 4 H, Ar H); IR (CHCl_3) 3590, 3500 (OH), 2930, 1510, 1450, 1370, 1230, 1180, 1100, 1040, 830 cm^{-1} ; mass spectrum, m/z (rel intensity) 197 (P^+ + 1, 7), 196 (P^+ , 55), 110 (78), 73 (42), 59 (100). Anal. Calcd for $\text{C}_{11}\text{H}_{16}\text{O}_3$: C, 67.32; H, 8.22. Found: C, 67.42; H, 8.33.

Analytical Data for the Methoxy and Propoxy Phenols Follow. *p*-[(*S*)-2-Methoxypropoxy]phenol: white solid (mp 77.5–78.5 °C); ^1H NMR (90 MHz, CDCl_3) δ 1.23 (d, 3 H, J = 6.3 Hz, $\text{R-OCH}_2\text{CH}(\text{CH}_3)\text{OR}$), 3.43 (s, 3 H, ROCH_3), 3.80 (m, 3 H, $\text{R-OCH}_2\text{CH}(\text{CH}_3)\text{OR}$), 6.5 (s, 1 H, ArOH), 6.78 (s, 4 H, Ar H); ^{13}C NMR (CDCl_3) δ 16.36, 56.64, 72.19, 75.61, 115.85, 116.10, 150.13, 152.64; IR (CHCl_3) 3575, 3322, 2975, 1600, 1510, 1451, 1378, 1160, 1100, 1040, 825 cm^{-1} ; mass spectrum, m/z (rel intensity) 182 (P^+ , 60), 110 (83), 73 (100). Anal. Calcd for $\text{C}_{10}\text{H}_{14}\text{O}_3$: C, 65.92; H, 7.74. Found: C, 65.72; H, 7.96.

p-[(*S*)-2-Propoxypropoxy]phenol: colorless liquid; ^1H NMR (90 MHz, CDCl_3) δ 0.82 (t, 3 H, J = 6.3 Hz, $\text{ROCH}_2\text{CH}_2\text{CH}_3$), 1.24 (m, 5 H, $\text{ROCH}_2\text{CH}_2\text{CH}_3$ and $\text{ROCH}_2\text{CH}(\text{CH}_3)\text{OR}$), 3.44 (t, 2 H, J = 6.3 Hz, $\text{ROCH}_2\text{CH}_2\text{CH}_3$), 3.75 (m, 3 H, $\text{ROCH}_2\text{CH}(\text{CH}_3)\text{OR}$), 4.84 (s, 1 H, ArOH), 6.73 (s, 4 H, Ar H); IR (CHCl_3) 3600, 3350, 2950, 1740, 1600, 1520, 1460, 1380, 1240, 1110, 1050, 840 cm^{-1} ; mass spectrum, m/z (rel intensity) 210 (P^+ , 67), 110 (100). Anal. Calcd for $\text{C}_{12}\text{H}_{18}\text{O}_3$: C, 68.55; H, 8.63. Found: C, 68.31; H, 8.75.

Representative Procedure for Coupling of *p*-[(*S*)-2-Alkoxypropoxy]phenols with *p*-Alkoxybenzoyl Chlorides 15. 4'-[(*S*)-2-Ethoxypropoxy]phenyl 4-(*n*-Decyloxy)benzoate (1, R^1 = *n*-Decyl, R^2 = Ethyl). To a flask containing 43 mg (1.79 mmol) of oil-free sodium hydride was added 35 mL of dry THF and a solution of 350 mg (1.79 mmol) of *p*-[(*S*)-2-ethoxypropoxy]phenol in 10 mL of THF. After stirring for 15 min, a solution of 530 mg (1.79 mmol) of (*p*-*n*-decyloxy)benzoyl chloride was added. When the reaction was judged complete by TLC (\approx 18 h, product R_f 0.31 eluting with 9:1 hexanes/ethyl acetate), the reaction was quenched by addition of water, and the resulting aqueous phase was extracted with ether. The combined organic extracts were washed with 10% aqueous HCl, 5% aqueous NaOH, and brine, then dried, and filtered, and the solvent was stripped by rotary evaporation. The crude product was purified by flash chromatography to give 775 mg (95%) of 1 (R^1 = *n*-decyl, R^2 = ethyl) as a white solid showing the spectra reported below. In order to obtain material suitable for liquid crystal studies, however, several flash chromatographies, followed by recrystallization from ethanol and separate recrystallization from hexane, were required. For all of the measurements reported in this work, liquid crystal materials with a 0.5 °C isotropic-smectic A coexistence range were utilized: ^1H NMR (CDCl_3) δ 0.90 (t, 3 H, J = 7.4 Hz, $\text{ArOCH}_2\text{CH}_2[\text{CH}_2]_7\text{CH}_3$), 1.26 (m, 20 H, $\text{ArOCH}_2\text{CH}_2[\text{CH}_2]_7\text{CH}_3$, ROCH_2CH_3 , and $\text{R-OCH}_2\text{CH}(\text{CH}_3)\text{OR}$), 1.79 (m, 2 H, $\text{ArOCH}_2\text{CH}_2[\text{CH}_2]_7\text{CH}_3$), 3.62 (m, 2 H, ROCH_2CH_3), 3.82 (m, 2 H, $\text{ArOCH}_2\text{CH}_2[\text{CH}_2]_7\text{CH}_3$), 4.04 (m, 3 H, $\text{R-OCH}_2\text{CH}(\text{CH}_3)\text{OR}$), 6.95 (m, 4 H, hydroquinone Ar H), 7.08 (d, 2 H, J = 9.2 Hz, benzoate Ar H), 8.12 (d, 2 H, J = 9.2 Hz, benzoate Ar H); ^{13}C NMR (CDCl_3) δ 14.07, 15.66, 17.51, 22.69, 26.03, 29.18, 29.33, 29.39, 31.92, 64.74, 68.40, 72.37, 73.61, 114.37, 115.38, 121.89, 122.51, 132.22, 144.86, 156.68, 163.56, 165.22; IR (CHCl_3) 2930, 2860, 1720, 1605, 1505 cm^{-1} ; mass spectrum, m/z (rel intensity) 457 (P^+ , 9), 262 (62), 261 (100), 121 (76). Anal. Calcd for $\text{C}_{28}\text{H}_{40}\text{O}_5$: C, 73.65; H, 8.83. Found: C, 73.63; H, 8.83.

Analytical Data for Other Compounds 1 Follow. 4'-[(*S*)-2-Methoxypropoxy]phenyl 4-(*n*-Nonyloxy)benzoate (1, R^1 = *n*-Nonyl, R^2 = Methyl): ^1H NMR (CDCl_3) δ 0.80 (t, 3 H, J = 6.2 Hz, $\text{ArOCH}_2\text{CH}_2[\text{CH}_2]_6\text{CH}_3$), 1.24 (m, 15 H, $\text{ArOCH}_2\text{CH}_2[\text{CH}_2]_6\text{CH}_3$ and $\text{ROCH}_2\text{CH}(\text{CH}_3)\text{OR}$), 1.53 (m, 2 H, $\text{ArOCH}_2\text{CH}_2[\text{CH}_2]_6\text{CH}_3$), 3.46 (s, 3 H, ROCH_3), 3.82 (m, 2 H, $\text{ArOCH}_2\text{CH}_2[\text{CH}_2]_6\text{CH}_3$), 4.00 (m, 3 H, $\text{R-OCH}_2\text{CH}(\text{CH}_3)\text{OR}$), 7.00 (m, 4 H, hydroquinone Ar H), 7.05 (d, 2 H, J = 9.2 Hz, benzoate Ar H), 8.21 (d, 2 H, J = 9.2 Hz, benzoate Ar H); IR (CHCl_3) 2930, 2860, 1720, 1605, 1505 cm^{-1} ; mass spectrum, m/z (rel intensity) 429 (P^+ + 1, 17), 428 (P^+ , 53), 247 (100), 121 (73). Anal. Calcd for $\text{C}_{26}\text{H}_{36}\text{O}_5$: C, 72.87; H, 8.47. Found: C, 72.90; H, 8.42.

4'-[(*S*)-2-Ethoxypropoxy]phenyl 4-(*n*-Nonyloxy)benzoate (1, R^1 = *n*-Nonyl, R^2 = Ethyl): ^1H NMR (CDCl_3) δ 0.90 (t, 3 H, J = 7.4 Hz, $\text{ArOCH}_2\text{CH}_2[\text{CH}_2]_6\text{CH}_3$), 1.26 (m, 18 H, $\text{ArOCH}_2\text{CH}_2[\text{CH}_2]_6\text{CH}_3$, ROCH_2CH_3 , and $\text{R-OCH}_2\text{CH}(\text{CH}_3)\text{OR}$), 1.79 (m, 2 H, $\text{ArOCH}_2\text{CH}_2[\text{CH}_2]_6\text{CH}_3$), 3.62 (m, 2 H, ROCH_2CH_3), 3.82 (m, 2 H, $\text{ArOCH}_2\text{CH}_2[\text{CH}_2]_6\text{CH}_3$), 4.03 (m, 3 H, $\text{R-OCH}_2\text{CH}_2\text{CH}(\text{CH}_3)\text{OR}$), 6.94 (m, 4 H, hydroquinone Ar H), 7.08 (d, 2 H, J = 9.2 Hz, benzoate

Ar H), 8.11 (d, 2 H, J = 9.2 Hz, benzoate Ar H); IR (CHCl_3) 2930, 2860, 1720, 1605, 1505 cm^{-1} ; mass spectrum, m/z (rel intensity) 443 (P^+ + 1, 10), 442 (P^+ , 32), 248 (48), 247 (100), 121 (83). Anal. Calcd for $\text{C}_{27}\text{H}_{38}\text{O}_5$: C, 73.27; H, 8.65. Found: C, 73.19; H, 8.65.

4'-[(*S*)-2-Propoxypropoxy]phenyl 4-(*n*-Nonyloxy)benzoate (1, R^1 = *n*-Nonyl, R^2 = *n*-Propyl): ^1H NMR (CDCl_3) δ 0.88 (m, 6 H, $\text{ArOCH}_2\text{CH}_2[\text{CH}_2]_6\text{CH}_3$ and $\text{ROCH}_2\text{CH}_2\text{CH}_3$), 1.25 (m, 15 H, $\text{ArOCH}_2\text{CH}_2[\text{CH}_2]_6\text{CH}_3$ and $\text{R-OCH}_2\text{CH}(\text{CH}_3)\text{OR}$), 1.58 (m, 2 H, $\text{ROCH}_2\text{CH}_2\text{CH}_3$), 1.80 (m, 2 H, $\text{ArOCH}_2\text{CH}_2[\text{CH}_2]_6\text{CH}_3$), 3.50 (m, 2 H, $\text{ROCH}_2\text{CH}_2\text{CH}_3$), 3.82 (m, 2 H, $\text{ArOCH}_2\text{CH}_2[\text{CH}_2]_6\text{CH}_3$), 4.02 (m, 3 H, $\text{ROCH}_2\text{CH}(\text{CH}_3)\text{OR}$), 6.95 (m, 4 H, hydroquinone Ar H), 7.09 (d, 2 H, J = 9.2 Hz, benzoate Ar H), 8.11 (d, 2 H, J = 9.2 Hz, benzoate Ar H); IR (CHCl_3) 2930, 2860, 1720, 1605, 1505 cm^{-1} ; mass spectrum, m/z (rel intensity) 458 (P^+ + 1, 12), 457 (P^+ , 39), 248 (62), 247 (100), 121 (73). Anal. Calcd for $\text{C}_{28}\text{H}_{40}\text{O}_5$: C, 73.65; H, 8.83. Found: C, 73.87; H, 9.03.

4'-[(*S*)-2-Methoxypropoxy]phenyl 4-(*n*-Decyloxy)benzoate (1, R^1 = *n*-Decyl, R^2 = Methyl): ^1H NMR (90 MHz, CDCl_3) δ 0.87 (t, 3 H, J = 6.2 Hz, $\text{ArOCH}_2\text{CH}_2[\text{CH}_2]_7\text{CH}_3$), 1.29 (m, 17 H, $\text{ArOCH}_2\text{CH}_2[\text{CH}_2]_7\text{CH}_3$ and $\text{ROCH}_2\text{CH}(\text{CH}_3)\text{OR}$), 1.77 (m, 2 H, $\text{ArOCH}_2\text{CH}_2[\text{CH}_2]_7\text{CH}_3$), 3.45 (s, 3 H, ROCH_3), 3.75 (m, 1 H, $\text{R-OCH}_2\text{CH}(\text{CH}_3)\text{OR}$), 3.93 (m, 2 H, $\text{R-OCH}_2\text{CH}(\text{CH}_3)\text{OR}$), 4.03 (t, 2 H, $\text{ArOCH}_2\text{CH}_2[\text{CH}_2]_7\text{CH}_3$), 7.05 (m, 6 H, Ar H), 8.20 (d, 2 H, J = 9.2 Hz, benzoate Ar H); ^{13}C NMR (CDCl_3) δ 14.08, 16.8, 22.8, 26.1, 29.2, 29.38, 29.44, 29.6, 32.0, 57.0, 68.5, 72.1, 114.4, 115.4, 122.0, 122.6, 132.3, 145.0, 156.7, 163.6, 165.3; IR (CHCl_3) 2930, 2860, 1720, 1605, 1505 cm^{-1} ; mass spectrum, m/z (rel intensity) 442 (P^+ , 9), 261 (100). Anal. Calcd for $\text{C}_{27}\text{H}_{38}\text{O}_5$: C, 73.27; H, 8.65. Found: C, 73.34; H, 8.71.

4'-[(*S*)-2-Propoxypropoxy]phenyl 4-(*n*-Decyloxy)benzoate (1, R^1 = *n*-Decyl, R^2 = *n*-Propyl): ^1H NMR (CDCl_3) δ 0.89 (m, 6 H, $\text{ArOCH}_2\text{CH}_2[\text{CH}_2]_7\text{CH}_3$ and $\text{ROCH}_2\text{CH}_2\text{CH}_3$), 1.25 (m, 17 H, $\text{ArOCH}_2\text{CH}_2[\text{CH}_2]_7\text{CH}_3$ and $\text{R-OCH}_2\text{CH}(\text{CH}_3)\text{OR}$), 1.58 (m, 2 H, $\text{ROCH}_2\text{CH}_2\text{CH}_3$), 1.80 (m, 2 H, $\text{ArOCH}_2\text{CH}_2[\text{CH}_2]_7\text{CH}_3$), 3.50 (t, 2 H, J = 6.6 Hz, $\text{ROCH}_2\text{CH}_2\text{CH}_3$), 3.85 (m, 2 H, $\text{ArOCH}_2\text{CH}_2[\text{CH}_2]_7\text{CH}_3$), 4.01 (m, 3 H, $\text{ROCH}_2\text{CH}(\text{CH}_3)\text{OR}$), 6.96 (m, 4 H, hydroquinone Ar H), 7.09 (d, 2 H, J = 9.2 Hz, benzoate Ar H), 8.12 (d, 2 H, J = 9.2 Hz, benzoate Ar H); IR (CHCl_3) 2930, 2860, 1720, 1605, 1505 cm^{-1} ; mass spectrum, m/z (rel intensity) 471 (P^+ + 1, 11), 470 (P^+ , 33), 262 (75), 261 (100). Anal. Calcd for $\text{C}_{29}\text{H}_{42}\text{O}_5$: C, 74.01; H, 8.99. Found: C, 74.12; H, 9.10.

4'-[(*S*)-2-Methoxypropoxy]phenyl 4-(*n*-Undecyloxy)benzoate (1, R^1 = *n*-Undecyl, R^2 = Methyl): ^1H NMR (90 MHz, CDCl_3) δ 0.91 (t, 3 H, J = 6.2 Hz, $\text{ArOCH}_2\text{CH}_2[\text{CH}_2]_8\text{CH}_3$), 1.30 (m, 19 H, $\text{ArOCH}_2\text{CH}_2[\text{CH}_2]_8\text{CH}_3$ and $\text{R-OCH}_2\text{CH}(\text{CH}_3)\text{OR}$), 1.86 (m, 2 H, $\text{ArOCH}_2\text{CH}_2[\text{CH}_2]_8\text{CH}_3$), 3.47 (s, 3 H, ROCH_3), 3.75 (m, 1 H, $\text{R-OCH}_2\text{CH}(\text{CH}_3)\text{OR}$), 3.97 (m, 2 H, $\text{R-OCH}_2\text{CH}(\text{CH}_3)\text{OR}$), 4.07 (t, 2 H, $\text{ArOCH}_2\text{CH}_2[\text{CH}_2]_8\text{CH}_3$), 7.10 (m, 6 H, Ar H), 8.25 (d, 2 H, J = 9.2 Hz, benzoate Ar H); ^{13}C NMR (CDCl_3) δ 13.9, 16.4, 22.5, 25.8, 28.9, 29.2, 29.4, 31.7, 56.7, 68.0, 71.5, 75.0, 114.0, 114.9, 121.4, 122.3, 131.9, 144.4, 156.2, 163.2, 164.9; IR (CHCl_3) 2930, 2860, 1720, 1605, 1505 cm^{-1} ; mass spectrum, m/z (rel intensity) 456 (P^+ , 10), 275 (100). Anal. Calcd for $\text{C}_{28}\text{H}_{40}\text{O}_5$: C, 73.65; H, 8.83. Found: C, 73.62; H, 8.90.

4'-[(*S*)-2-Ethoxypropoxy]phenyl 4-(*n*-Undecyloxy)benzoate (1, R^1 = *n*-Undecyl, R^2 = Ethyl): ^1H NMR (CDCl_3) δ 0.89 (t, 3 H, J = 7.5 Hz, $\text{ArOCH}_2\text{CH}_2[\text{CH}_2]_8\text{CH}_3$), 1.24 (m, 22 H, $\text{ArOCH}_2\text{CH}_2[\text{CH}_2]_8\text{CH}_3$, ROCH_2CH_3 , and $\text{ROCH}_2\text{CH}(\text{CH}_3)\text{OR}$), 1.79 (m, 2 H, $\text{ArOCH}_2\text{CH}_2[\text{CH}_2]_8\text{CH}_3$), 3.61 (m, 2 H, ROCH_2CH_3), 3.81 (m, 2 H, $\text{ArOCH}_2\text{CH}_2[\text{CH}_2]_8\text{CH}_3$), 4.01 (m, 3 H, $\text{ROCH}_2\text{CH}(\text{CH}_3)\text{OR}$), 6.92 (m, 4 H, hydroquinone Ar H), 7.08 (d, 2 H, J = 9.2 Hz, benzoate Ar H), 8.11 (d, 2 H, J = 9.2 Hz, benzoate Ar H); IR (CHCl_3) 2930, 2860, 1720, 1605, 1505 cm^{-1} ; mass spectrum, m/z (rel intensity) (P^+ , 15), 276 (55), 275 (100), 121 (91). Anal. Calcd for $\text{C}_{29}\text{H}_{42}\text{O}_5$: C, 74.00; H, 9.00. Found: C, 74.25; H, 9.12.

4'-[(*S*)-2-Propoxypropoxy]phenyl 4-(*n*-Undecyloxy)benzoate (1, R^1 = *n*-Undecyl, R^2 = *n*-propyl): ^1H NMR (CDCl_3) δ 0.89 (m, 6 H, $\text{ArOCH}_2\text{CH}_2[\text{CH}_2]_8\text{CH}_3$ and $\text{ROCH}_2\text{CH}_2\text{CH}_3$), 1.25 (m, 19 H, $\text{ArOCH}_2\text{CH}_2[\text{CH}_2]_8\text{CH}_3$ and $\text{R-OCH}_2\text{CH}(\text{CH}_3)\text{OR}$), 1.58 (m, 2 H, $\text{ROCH}_2\text{CH}_2\text{CH}_3$), 1.80 (m, 2 H, $\text{ArOCH}_2\text{CH}_2[\text{CH}_2]_8\text{CH}_3$), 3.50 (t, 2 H, J = 6.58 Hz, $\text{ROCH}_2\text{CH}_2\text{CH}_3$), 3.85 (m, 2 H, $\text{ArOCH}_2\text{CH}_2[\text{CH}_2]_8\text{CH}_3$), 4.01 (m, 3 H, $\text{ROCH}_2\text{CH}(\text{CH}_3)\text{OR}$), 6.96 (m, 4 H, hydroquinone Ar H), 7.09 (d, 2 H, J = 9.2 Hz, benzoate Ar H), 8.11 (d, 2 H, J = 9.2 Hz, benzoate Ar H); IR (CHCl_3) 2930, 2860, 1720, 1605, 1505 cm^{-1} ; mass spectrum, m/z (rel intensity) 484 (P^+ , 21), 275 (100), 121 (83). Anal. Calcd for $\text{C}_{30}\text{H}_{44}\text{O}_5$: C, 74.34; H, 9.15. Found: C, 74.60; H, 9.10.

4'-[(*S*)-2-Methoxypropoxy]phenyl 4-(*n*-Dodecyloxy)benzoate (1, R^1 = *n*-Dodecyl, R^2 = Methyl): ^1H NMR (90 MHz, CDCl_3) δ 0.88 (t, 3 H, J = 6.2 Hz, $\text{ArOCH}_2\text{CH}_2[\text{CH}_2]_9\text{CH}_3$), 1.29 (m, 21 H, $\text{ArOCH}_2\text{CH}_2[\text{CH}_2]_9\text{CH}_3$ and $\text{ROCH}_2\text{CH}(\text{CH}_3)\text{OR}$), 1.80 (m, 2 H, $\text{ArOCH}_2\text{CH}_2[\text{CH}_2]_9\text{CH}_3$), 3.51 (s, 3 H, ROCH_3), 3.77 (m, 1 H, $\text{ROCH}_2\text{CH}(\text{CH}_3)\text{OR}$), 3.92 (m, 2 H, $\text{ROCH}_2\text{CH}(\text{CH}_3)\text{OR}$), 4.00 (m, 2

H, $\text{ArOCH}_2[\text{CH}_2]_9\text{CH}_3$), 7.03 (m, 6 H, Ar H), 8.18 (d, 2 H, $J = 9.2$ Hz, benzoate Ar H); ^{13}C NMR (CDCl_3) δ 13.9, 16.4, 22.5, 25.8, 28.9, 29.2, 29.4, 31.7, 56.6, 68.0, 17.5, 75.0, 114.0, 114.9, 115.2, 121.4, 122.2, 131.9, 144.4, 156.2, 163.2, 164.9; IR (CHCl_3) 2930, 2960, 1720, 1605, 1505 cm^{-1} ; mass spectrum, m/z (rel intensity) 471 ($\text{P}^+ + 1$, 17), 470 (P^+ , 45), 291 (51), 290 (100). Anal. Calcd for $\text{C}_{29}\text{H}_{42}\text{O}_5$: C, 74.00; H, 9.00. Found: C, 74.22; H, 9.15.

4'-[(*S*)-2-Ethoxypropoxy]phenyl 4-(*n*-Dodecyloxy)benzoate (**1**, $\text{R}^1 = n\text{-Dodecyl}$, $\text{R}^2 = \text{Ethyl}$): ^1H NMR (CDCl_3) δ 0.89 (t, 3 H, $J = 7.5$ Hz, $\text{ArOCH}_2\text{CH}_2[\text{CH}_2]_9\text{CH}_3$), 1.24 (m, 24 H, $\text{ArOCH}_2\text{CH}_2[\text{CH}_2]_9\text{CH}_3$, ROCH_2CH_3 , and $\text{ROCH}_2\text{CH}[\text{CH}_3]\text{OR}$), 1.79 (m, 2 H, $\text{ArOCH}_2\text{CH}_2[\text{CH}_2]_9\text{CH}_3$), 3.61 (m, 2 H, ROCH_2CH_3), 3.81 (m, 2 H, $\text{ArOCH}_2\text{CH}_2[\text{CH}_2]_9\text{CH}_3$), 4.01 (m, 3 H, $\text{ROCH}_2\text{CH}[\text{CH}_3]\text{OR}$), 6.92 (m, 4 H, hydroquinone Ar H), 7.08 (d, 2 H, $J = 9.2$ Hz, benzoate Ar H), 8.11 (d, 2 H, $J = 9.2$ Hz, benzoate Ar H); ^{13}C NMR (CDCl_3) δ 14.07, 15.66, 17.51, 22.70, 26.04, 29.18, 29.37, 29.39, 29.59, 29.61, 29.66, 31.95, 63.42, 64.75, 72.41, 73.63, 114.39, 115.40, 121.93, 122.52, 132.23, 144.89, 156.10, 163.58, 165.23; IR (CHCl_3) 2930, 2860, 1720, 1605, 1505 cm^{-1} . Anal. Calcd for $\text{C}_{30}\text{H}_{44}\text{O}_5$: C, 74.34; H, 9.15. Found: C, 74.26; H, 8.96.

4'-[(*S*)-2-Propoxypropoxy] 4-(*n*-Dodecyloxy)benzoate (**1**, $\text{R}^1 = n\text{-Dodecyl}$, $\text{R}^2 = n\text{-Propyl}$): ^1H NMR (CDCl_3) δ 0.89 (m, 6 H, $\text{ArOCH}_2\text{CH}_2[\text{CH}_2]_9\text{CH}_3$, and $\text{ROCH}_2\text{CH}_2\text{CH}_3$), 1.25 (m, 21 H, $\text{ArOCH}_2\text{CH}_2[\text{CH}_2]_9\text{CH}_3$ and $\text{ROCH}_2\text{CH}[\text{CH}_3]\text{OR}$), 1.58 (m, 2 H, $\text{ROCH}_2\text{CH}_2\text{CH}_3$), 1.80 (m, 2 H, $\text{ArOCH}_2\text{CH}_2[\text{CH}_2]_9\text{CH}_3$), 3.50 (t, 2 H, $J = 6.58$ Hz, $\text{ROCH}_2\text{CH}_2\text{CH}_3$), 3.85 (m, 2 H, $\text{ArOCH}_2\text{CH}_2[\text{CH}_2]_9\text{CH}_3$), 4.01 (m, 3 H, $\text{ROCH}_2\text{CH}[\text{CH}_3]\text{OR}$), 6.96 (m, 4 H, hydroquinone Ar H), 7.09 (d, 2 H, $J = 9.2$ Hz, benzoate Ar H), 8.11 (d, 2 H, $J = 9.2$ Hz, benzoate

Ar H); IR (CHCl_3) 2930, 2860, 1720, 1605, 1505 cm^{-1} ; mass spectrum m/z (rel intensity) 499 ($\text{P}^+ + 1$, 19), 498 (P^+ , 38), 291 (47), 290 (100). Anal. Calcd for $\text{C}_{31}\text{H}_{46}\text{O}_5$: C, 74.66; H, 9.30. Found: C, 74.36; H, 9.20.

Acknowledgment. We thank the National Science Foundation (Grant No. DMR-8219259) for financial support of this work. We also thank Rohini T. Vohra, Göran Lindsten, and Homaune A. Razavi (Department of Chemistry and Biochemistry, University of Colorado) and Michael D. Wand (Displaytech, Inc., Boulder, CO) for their help with the synthesis of materials, and Jiuzhi Xue and Devendra S. Parmar (Department of Physics, University of Colorado) for help with physical measurements.

Registry No. **1** ($\text{R}^1 = n\text{-decyl}$; $\text{R}^2 = \text{ethyl}$), 103239-85-6; **1** ($\text{R}^1 = n\text{-nonyl}$; $\text{R}^2 = \text{methyl}$), 103239-86-7; **1** ($\text{R}^1 = n\text{-nonyl}$; $\text{R}^2 = \text{ethyl}$), 103239-87-8; **1** ($\text{R}^1 = n\text{-nonyl}$; $\text{R}^2 = n\text{-propyl}$), 103239-88-9; **1** ($\text{R}^1 = n\text{-decyl}$; $\text{R}^2 = \text{methyl}$), 103239-89-0; **1** ($\text{R}^1 = n\text{-decyl}$; $\text{R}^2 = n\text{-propyl}$), 103239-90-3; **1** ($\text{R}^1 = n\text{-undecyl}$; $\text{R}^2 = \text{methyl}$), 103239-91-4; **1** ($\text{R}^1 = n\text{-undecyl}$; $\text{R}^2 = \text{ethyl}$), 103239-92-5; **1** ($\text{R}^1 = n\text{-undecyl}$; $\text{R}^2 = n\text{-propyl}$), 103239-93-6; **1** ($\text{R}^1 = n\text{-dodecyl}$; $\text{R}^2 = \text{methyl}$), 103239-94-7; **1** ($\text{R}^1 = n\text{-dodecyl}$; $\text{R}^2 = \text{ethyl}$), 103239-95-8; **1** ($\text{R}^1 = n\text{-dodecyl}$; $\text{R}^2 = n\text{-propyl}$), 103239-96-9; **12**, 103239-97-0; **13**, 103239-98-1; **14** ($\text{R}^2 = \text{ethyl}$), 103239-99-2; **14** ($\text{R}^2 = \text{methyl}$), 103240-00-2; **14** ($\text{R}^2 = n\text{-propyl}$), 103240-01-3; *p*-[(*S*)-2-ethoxypropoxy]phenol, 103240-02-4; *p*-[(*S*)-2-methoxypropoxy]phenol, 103240-03-5; *p*-[(*S*)-2-propoxypropoxy]phenol, 103240-04-6.

Stereocontrolled Asymmetric Total Synthesis of Protomycinolide IV

Keisuke Suzuki,* Katsuhiko Tomooka, Eiji Katayama, Takashi Matsumoto, and Gen-ichi Tsuchihashi*

Contribution from the Department of Chemistry, Faculty of Science and Technology, Keio University, Hiyoshi, Yokoyama 223, Japan. Received February 4, 1986

Abstract: Stereocontrolled asymmetric total synthesis of protomycinolide IV (**1**) was achieved, based on the organo-aluminum-promoted stereospecific pinacol-type 1,2-rearrangement. Two chiral fragments, C(1)–C(9) and C(11)–C(17) portions, were constructed from a common chiral starting material, (*S*)-ethyl lactate. High diastereoselectivity of the nucleophilic attack on the Me_3Si -bearing α -methyl- β,γ -unsaturated carbonyl compounds was fully utilized for establishing the chiral centers at C(5) and C(6) relative to C(4) and C(15) relative to C(14). For the stereocontrol of the Me substituent at C(8), two methods were newly devised: (i) thermodynamic equilibration of δ -lactone **16** and (ii) acid-catalyzed stereoselective cyclization of ketene dithioacetal possessing an internal hydroxyl group.

Recent interest in the total synthesis of macrolide or ionophore antibiotics invoked rapid progress of the stereoregulating method for the synthesis of acyclic molecules.¹ In this conjunction, a number of efficient methods have been recently devised,^{2a} such as the stereoselective aldol condensation^{2b} etc., which serve well for the control of the acyclic stereochemistry, both in enantio- and diastereomeric senses. However, there is room for further development, seeking generality and flexibility against structural diversity. Our recent investigation in this area revealed a viable approach based on 1,2-rearrangement in acyclic systems, which proved to be highly efficient in light of its excellent enantiospecificity.

Scheme I illustrates key features of our approach: Pinacol-type 1,2-rearrangement of the lactate-derived mesylate **1** proceeded with a full inversion of the C–OMs stereocenter to give *enan-*

tiomerically pure α -chiral ketone **II**. The use of organoaluminums as the Lewis-acidic reaction promotor is essential for this success where Al-chelate **VIII** is postulated as an intermediate. A related chelate intermediate, reductively generated by reaction of DIBAL with **IV**, undergoes 1,2-rearrangement leading to the chiral aldehyde **V**. These 1,2-migration reactions effect net chirality transfer from the naturally abundant "C–O asymmetry" (e.g., carbohydrates, lactic or tartaric acid) into the chiral synthons possessing "C–C asymmetry", as can be seen in **II** or **V**.

These chiral synthons, α -methyl- β,γ -unsaturated carbonyls, are characterized by their high enantiomeric purity, but equally important is their inherent Cram selectivity observed when they are subjected to a nucleophilic attack upon the carbonyl carbon: Reduction of ketone **II** gives *threo*-alcohol **III** with high selectivity. *Erythro* isomer **VI** is also accessible by nucleophilic reaction with aldehyde **V**,³ as anticipated by the Felkin–Anh model **IX**,⁴ where

(1) Masamune, S.; Choy, W.; Peterson, J. S.; Sita, L. R. *Angew. Chem., Int. Ed. Engl.* **1985**, *24*, 1–76. Paterson, I.; Mansuri, M. M. *Tetrahedron* **1985**, *41*, 3569–3624.

(2) (a) Review: Morrison, J. D. *Asymmetric Synthesis*; Academic: New York, 1984. (b) Reviews: Evans, D. A.; Nelson, J. V.; Taber, T. R. *Top. Stereochem.* **1982**, *13*, 1–115. Mukaiyama, T. *Org. React.* **1982**, *28*, 203–331. Heathcock, C. H. In ref 2a; Vol. 3, pp 111–212.

(3) For *threo/erythro* nomenclature, Heathcock's convention was used: Heathcock, C. H.; Buse, C. T.; Kleschick, W. A.; Pirrung, M. C.; Sohn, J. E.; Lampe, J. J. *Org. Chem.* **1980**, *45*, 1066–1081. The numbering system used for **1** is utilized in the discussion of all synthetic intermediates. The proper IUPAC numbering is found in the Experimental Section.